SECTION 22 PLANNING ASSISTANCE TO STATES AND TRIBES PHASE I

LAKE OSAKIS SEDIMENT ANALYSIS

APPENDIX A: CE-QUAL-W2 – Water Quality Model

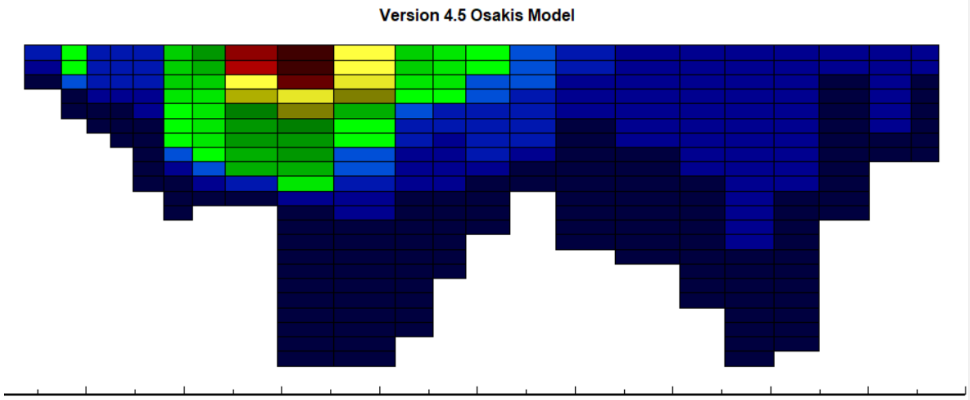

June 2026

US Army Corps of Engineers ®

Prepared by:
U.S. Army Corps of Engineers
St. Paul District
332 Minnesota St., Suite E1500
St. Paul, MN 55101

Lake Osakis CE-QUAL-W2 Water Quality Model

1 Introduction

The Lake Osakis CE-QUAL-W2 modeling study was undertaken by the U.S. Army Corps of Engineers (USACE), St. Paul District, in cooperation with the Sauk River Watershed District (SRWD) and Houston Engineering, Inc. (HEI). This modeling effort directly supports the Alternatives Analysis study for the Lake Osakis Watershed on behalf of the SRWD.

1.1 Background

The Lake Osakis study was initiated under the Lake Osakis Alternatives Analysis - Planning Assistance to States (PAS) program, with a specific focus on Miller Bay. Local stakeholders have identified Miller Bay as an area of significant concern due to the rapid accumulation of sediment and organic material. There is widespread concern that this deposition is degrading the overall ecological and recreational function of Lake Osakis, and that the Judicial Ditch #2 (JD2) drainage system is the primary contributor of this material.

To address these concerns, multiple stakeholders seek to understand the origin, transport, and deposition of materials entering Miller Bay, as well as their broader impacts on the lake's water quality and hydrodynamic behavior.

The core objectives of this PAS planning effort are to:

- Establish Baseline Conditions: Quantify the sources and transport of materials deposited in Lake Osakis and evaluate their impacts on overall lake function.
- Evaluate Management Alternatives: Set realistic water quality goals and identify feasible watershed or in-lake restoration projects to achieve them.
- Assess Feasibility: Evaluate the regulatory, construction, and long-term operations and maintenance (O&M) feasibility of the proposed alternatives.

To meet these objectives, a high-resolution hydrodynamic and water quality model was required to simulate the complex interactions between watershed transport and in-lake response.

1.2 CE-QUAL-W2 Model

As part of the existing condition assessment, the USACE was directed to develop a Lake Response Model and Material Mass Balance. While initial planning envisioned a simplified, spatially-averaged BATHTUB model, technical coordination in late 2023 led the project team to transition to the CE-QUAL-W2 modeling framework. CE-QUAL-W2 is a two-dimensional (longitudinal/vertical), laterally averaged hydrodynamic and water quality model. This framework is uniquely suited for relatively long, narrow waterbodies that exhibit thermal stratification, density currents, and complex internal nutrient loading.

Under this collaborative approach:

- USACE provided overall modeling oversight, developed the model grid, calibrated the hydrodynamics and water quality, and ran the alternative scenarios.
- HEI (under the direction of the SRWD) compiled and prepared the input data, including detailed bathymetric grids, sediment core incubation data to estimate internal loading rates, and watershed boundary conditions.

The watershed boundary conditions were derived from the State of Minnesota’s Hydrological Simulation Program – FORTRAN (HSPF) model, which provided daily flow and water quality inputs for the tributary streams. The transition to CE-QUAL-W2 significantly enhanced the project's capability to model the spatially distinct impacts of JD2 inflows on Miller Bay, simulate summer thermal stratification, and evaluate the specific ecological benefits of proposed restoration alternatives—such as wetland restorations, sediment basins, and channel modifications.

1.3 Study site

Lake Osakis is a large, eutrophic glacial lake located in west-central Minnesota within the Upper Sauk River watershed (HUC 07010202) (Figure 1). It is a dimictic lake, meaning it undergoes thermal stratification in the summer and winter, mixing completely in the spring and fall. This stratification is a key driver of its water quality dynamics.

Lake Osakis supports a popular walleye fishery but frequently experiences elevated nutrient concentrations, dense algal growth, and periodic hypolimnetic oxygen depletion during summer stratification. These conditions have led to eutrophication concerns and the development of a nutrient total maximum daily load (TMDL) study by the Minnesota Pollution Control Agency (MPCA, 2023).

Figure 1. Lake Osakis Vicinity and Location Map.

1.3.1 Headwater and Tributary Lake Descriptions

Major inflows include Judicial Ditch #2 (JD2) and several smaller agricultural drainage systems, while the outlet flows south through Osakis Creek to the Sauk River. The watershed is dominated by cultivated cropland (~65%), with grassland-pasture (20%), forest (10%), and developed/urban land uses (5%) contributing the remainder (USGS NLCD, 2019). The subwatersheds that contribute to Lake Osakis are shown in Figure 2. Lake Osakis' total contributing watershed spans 88,722 acres. The major inflows contributing to the lake's water budget include JD2 and Smith Lake (30%), direct watershed runoff (23%), Faille Lake (17%), Smith Lake headwaters (13%), Little Osakis Lake (10%), and Maple Lake (7%). Table 1 details the morphometric and hydrologic characteristics of Lake Osakis and the two main upstream water bodies, Smith and Falle Lakes.

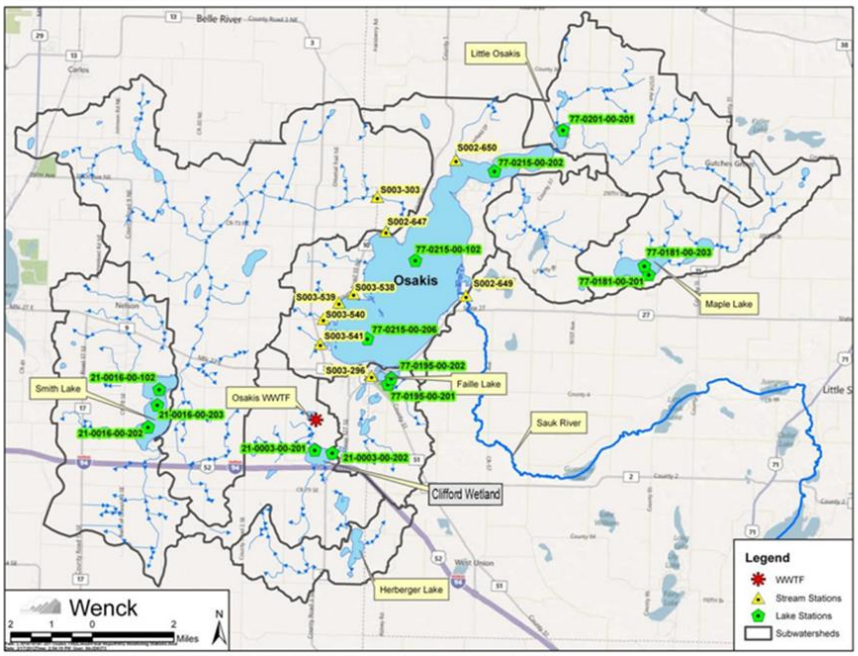

Figure 2.4. Lake and stream water quality sampling locations in the Osakis Lake Watershed.

Figure 2. Watershed Sub-basins and Tributary Drainage Areas for Lake Osakis.

Table 1. Morphometric and Hydrologic Characteristics of the Study Waterbodies

Parameter	**Smith Lake**	**Faille Lake**	**Lake Osakis**
Surface Area (acres / km^2)	550 / 2.2	78 / 0.3	6,405 / 25.9
Maximum Depth (ft / m)	30.0 / 9.1	7.0 / 2.1	74.8 / 22.8
Mean Depth (ft / m)	14.4 / 4.4	3.6 / 1.1	18.0 / 5.5
Volume (ac-ft / million m^3)	7,928 / 9.8	281 / 0.35	115,068 / 141.9
Hydraulic Residence Time	1.9 years	18 days (0.05 yrs)	~5.0 years
Watershed Area (acres / km^2)	11,931 / 48.3	14,722 / 59.6	88,722 / 359.0
Littoral Area fraction (%)	~50%	100%	~44%
Inflow Contribution to Osakis	~13% (via JD2)	~17% (via Blacks Channel)	N/A (Receives upstream loads)

1.3.2 Morphometric Interpretation

The physical structure of Lake Osakis plays a defining role in its water quality challenges. Morphometric indices derived from the 2024 bathymetric survey reveal a complex basin dynamic governed by competing physical forces (Table 2).

Table 2. Key Morphometric Indices for Lake Osakis and Their Physical Implications

Metric	**Value**	**Limnological Significance**	**Impact on Lake Osakis**
Shoreline Development Index (SDI)	1.5	Indicates a moderately irregular shoreline.	Creates sheltered embayments like Miller Bay that behave independently from the main lake basin.
Relative Depth (Z_r)	0.45%	Low ratio; indicates high vulnerability to wind-induced shear stress.	Makes the lake susceptible to sudden mixing (destratification) during high-wind summer storms.
Volume Development (D_v)	0.72	Represents a V-shaped basin with steep underwater slopes.	Concentrates water volume in deeper layers, promoting stable thermal stratification that isolates the cold hypolimnion.

2 CE-QUAL-W2 Model Development

2.1 CE-QUAL-W2 Model Background

CE-QUAL-W2 is a two-dimensional, longitudinal/vertical, hydrodynamic and water quality model for rivers, estuaries, lakes, reservoirs and river basin systems. Some of the model capabilities include hydrodynamic modeling, water quality, long term simulations, head boundary conditions, multiple branches, multiple water bodies, variable grid spacing, coupled water quality with hydrodynamics, auto stepping, restart provision, layer/segment addition and subtraction, multiple inflows and outflows, ice cover calculations, selective withdrawal calculations, and time-varying boundary conditions. The governing equations are laterally averaged which may be inappropriate for large water bodies exhibiting significant lateral variations in water quality.

CE-QUAL-W2 was originally developed in the 1970s as a hydrodynamic model, the Laterally Averaged Reservoir Model. Over the last several decades, the development of the model has been led by the USACE and Portland State University (PSU). CE-QUAL-W2 Version 4.5, released by PSU, (S. A. Wells 2025) was used in this project to model Lake Osakis.

Data requirements for successful application of the CE-QUAL-W2 model depend on what parameters are simulated. At a minimum for flow and temperature models, data required includes geometric data (bathymetric x-y-z data), initial conditions and boundary conditions (temperature and flow), hydraulic parameters, kinetic parameters, meteorological data and calibration data. Meteorological data includes air temperature, dew point temperature (or relative humidity), wind speed and direction, cloud cover and/or solar radiation. If the model contains hydraulic structures, flow rates need to be measured or calculated using structure details such as physical dimensions and or rating curves. For modeling water quality, parameters involved with the fate and transport of the parameter(s) of interest is/are necessary. For this study, where the focus is on the interrelationships of the physical lake characteristics and nutrient availability due to the dynamics of large suspended sediment loads from JD 2, boundary and calibration data of chlorophyll a, dissolved oxygen, organic matter and nutrients (e.g., NH_4, NO_3, and PO_4) were required.

2.2 Model Bathymetry

The CE-QUAL-W2 model grid for Lake Osakis was developed from high-resolution bathymetric data collected by Houston Engineering, Inc. (HEI) in 2024. This recent survey offers a significantly more detailed representation of the basin's features than legacy datasets, particularly within the shallow western basin and the complex channels of Miller Bay. Model grid geometry—including segment volumes, surface areas, and widths—was calculated directly from this XYZ dataset.

2.2.1 Horizontal Grid

To accurately represent the distinct hydrodynamic characteristics of the lake, the model was configured with a two-branch grid (Figure 3):

- Branch 1 (Main Lake): The main body of Lake Osakis was divided into 25 longitudinal segments, each approximately 300-800 m in length. These segments are numbered from upstream (west, near the primary inflows) to downstream (east, past the Sauk River outlet).
- Branch 2 (Miller Bay): Miller Bay, an area of specific concern, was represented as a tributary branch consisting of 4 longitudinal segments. This branch connects to the main

lake at segment 16, allowing the model to explicitly simulate the exchange of water and materials between the bay and the main lake.

2.2.2 Vertical Grid

Vertically, the model was divided into 25 layers, each with a uniform thickness of 1.0 meter (Figure 4).

2.2.3 Model Grid Configuration Summary

For quick reference, the key model grid parameters are summarized in Table 3 below.

Table 3. Model Grid Configuration Summary

Parameter	**Configuration**
Number of Branches	2
Main Branch Segments (Branch 1)	25
Miller Bay Segments (Branch 2)	4
Segment Length (approx.)	300-800 m
Total Vertical Layers	25
Layer Thickness	1.0 m

2.2.4 Geometric Validation

Figure 5 provides a critical validation of the model's geometric setup by comparing its hypsographic curves (depth-area and depth-volume relationships) to those derived from the high-resolution 2024 bathymetric survey.

Specifically, this analysis plots the "true" morphometry calculated from the complete HEI 2024 dataset (blue lines) against the relationships calculated directly from the discretized CE-QUAL-W2 model grid (red lines). The red and blue curves align almost perfectly, revealing excellent agreement between the model grid's geometry and the actual lake basin.

This close match is crucial because it confirms that the model grid accurately represents the key physical properties of the basin:

- Mass Balance: It ensures the model represents the true lake volume, which is vital for correct constituent mass-balance calculations.

- Boundary Fluxes: It validates the surface area at varying elevations, which is necessary for calculating surface heat exchange, wind shear, and evaporation.
- Thermal Dynamics: It confirms that the vertical distribution of volume and area is accurate, which is essential for simulating thermal stratification and vertical hydrodynamics.

Ultimately, this validation proves that the model's discretization is robust, lending high confidence to the subsequent predictive simulations.

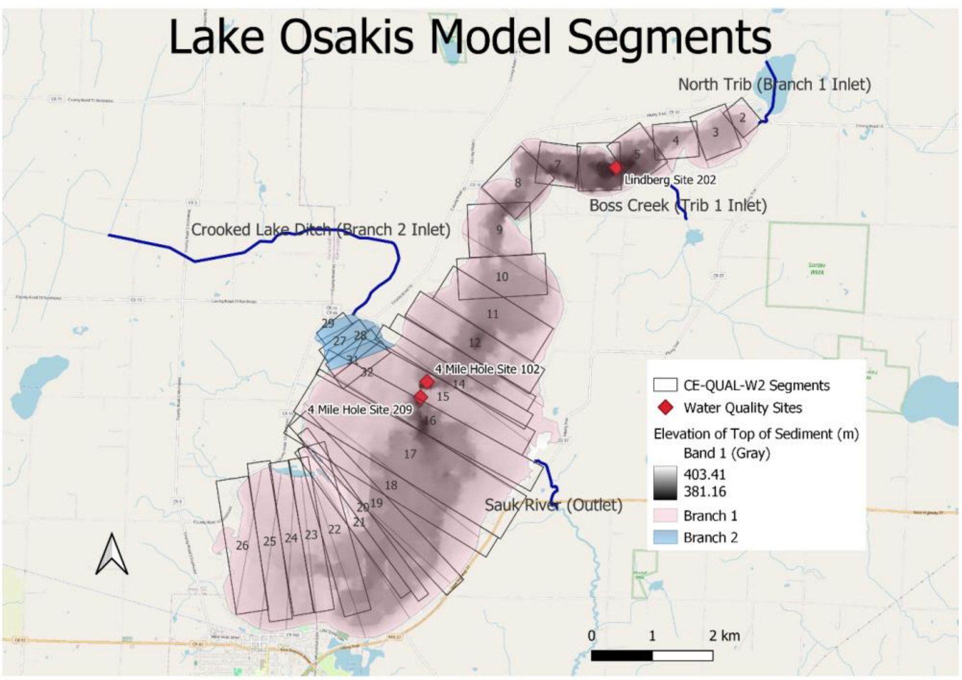

Figure 3. Lake Osakis CE-QUAL-W2 Model Grid Segmentation

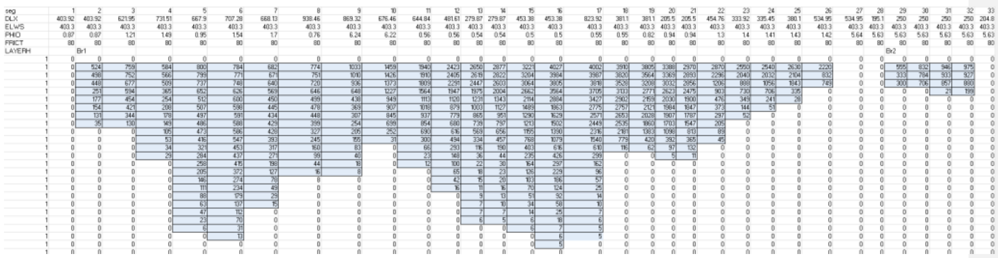

Figure 4. CE-QUAL-W2 Vertical Layer Discretization Shown in Model Control File

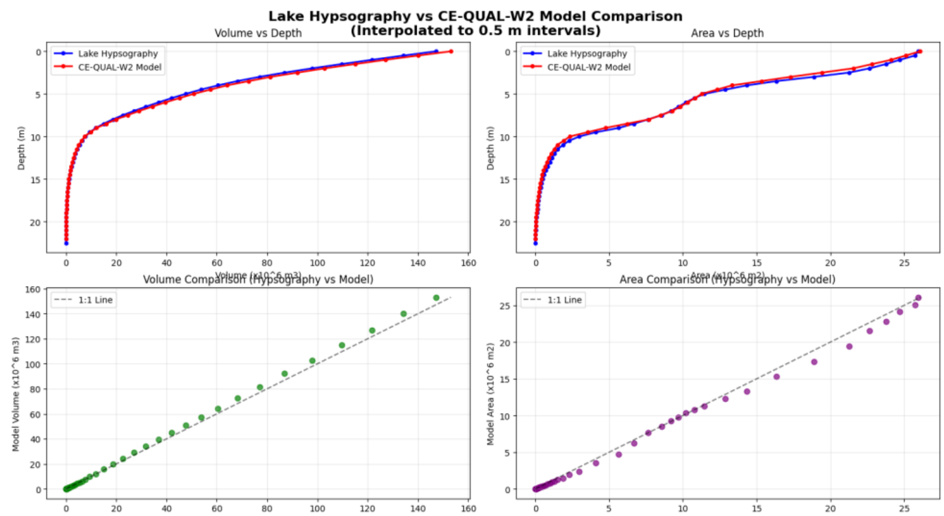

Figure 5. Comparison of Model Grid Geometry to Observed Lake Hypsography

2.3 Boundary Conditions

The CE-QUAL-W2 model requires time-series data for all external inputs (boundary conditions) and a definition of the lake's state at the beginning of the simulation period (initial conditions).

The model was run for the full period from January 1, 1996, to December 31, 2015. The year 2012 was selected as the primary calibration period due to the availability of comprehensive, concurrent monitoring data. The remaining years in the 1996-2015 timeframe were used for the model validation, confirming its ability to reproduce lake dynamics under a wide range of hydrologic and meteorological conditions.

2.3.1 Hydrologic Boundary Conditions

The hydrologic boundary conditions, which define the primary inflows of water to Lake Osakis, were derived from the State of Minnesota's HSPF watershed model for the Sauk River Basin. The model was configured with three main tributary inflows, each with its own sub-daily time series of flow data for the 1996-2015 simulation period.

The hydrographs for these inflows, shown in the figures below, are characteristic of streams in this agricultural region. They exhibit a "flashy" response, with sharp, high-flow peaks corresponding to precipitation and snowmelt events, followed by extended periods of low baseflow.

2.3.1.1 Tributary Descriptions:

Crooked Lake Ditch (Inflow to Branch 2): As shown in its hydrograph (Figure 6), this tributary is the most significant source of inflow to the lake system. Corresponding to the Judicial Ditch 2 (JD2) system, it discharges into the Miller Bay (Branch 2 in the model). Its flow is highly variable and is the critical driver of hydrodynamics and sediment transport within the bay. During the simulation period, it frequently produced storm peaks exceeding 200 cfs (~6 cms), with a maximum simulated peak flow of over 1,300 cfs (~37 cms).

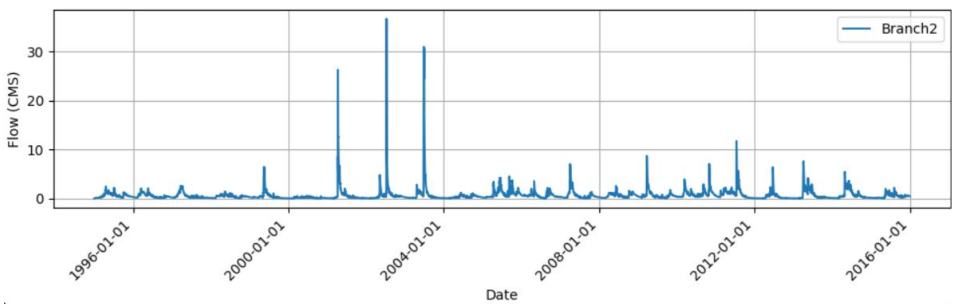

Figure 6. Inflow Hydrograph for Crooked Lake Ditch (Branch 2), 1996-2015.

North Branch (Inflow to Branch 1): The North Branch is the primary inflow to the main lake branch (Branch 1). While it contributes a substantial volume of water, its peak flows are generally lower than those from Crooked Lake Ditch. Its hydrograph (Figure 7) shows frequent storm peaks in the 35-70 cfs (1-2 cms) range, with a maximum simulated flow of over 200 cfs (~6 cms).

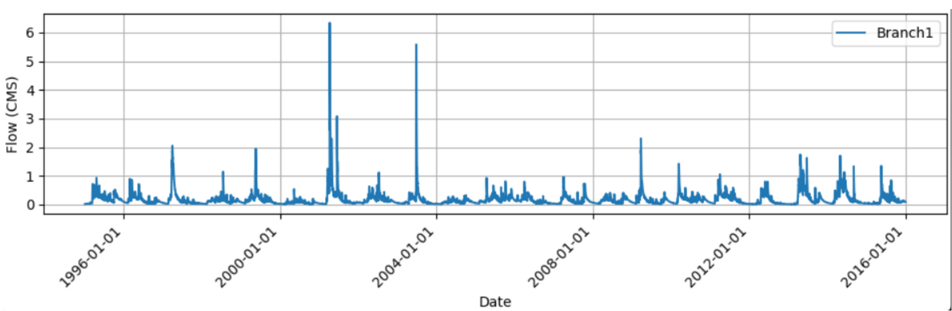

Figure 7. Inflow Hydrograph for North Branch (Branch 1), 1996-2015.

Boss Creek East (Tributary to Branch 1): Boss Creek East is a smaller tributary that discharges into the eastern, downstream portion of the main lake branch. As its hydrograph (Figure 8) indicates, it contributes a significantly lower volume of water compared to the other two inflows but did have a couple high peak flows around 300 cfs (~10 cms).

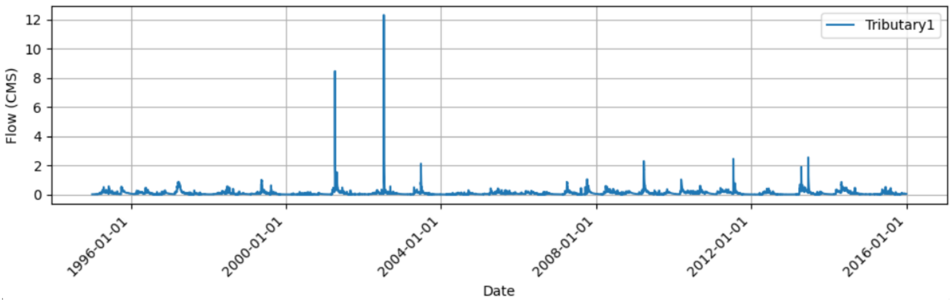

Figure 8. Inflow Hydrograph for Boss Creek East (Tributary 1), 1996-2015.

2.3.1.2 Importance for Modeling:

These inflows are the primary driver of external loading for water, sediment, and nutrients to the CE-QUAL-W2 model. The magnitude and timing of these flows—particularly the dominant discharge from Crooked Lake Ditch into Miller Bay—directly influence the lake's water balance, residence time, circulation patterns, and the delivery of pollutants that affect water quality and promote algal blooms. However, the significant residence time of Lake Osakis (~5 years) attenuates any in-lake water quality changes from external sources.

2.3.1.3 Hydrologic Analysis Summary

A statistical analysis was performed on the 20-year (1996-2015) hourly flow time series for the three primary tributaries, sourced from the MPCA's HSPF watershed model. The analysis confirms the "flashy," event-driven nature of these agricultural streams and quantifies the dominant contribution from the western watershed.

2.3.1.4 Comparative Flow Statistics

Table 4 below summarizes and compares the key flow statistics for each tributary. Crooked Lake Ditch is clearly the dominant source of inflow, contributing approximately 71% of the mean total flow to the lake.

Table 4. Inflow characteristics for Lake Osakis.

Statistic	**Crooked Lake Ditch (Branch 2)**	**North Tributary (Branch 1)**	**Boss Creek East (Trib. 1)**	**Total Combined**
Mean Flow (cfs)	23.3	6.1	3.3	32.7
Mean Flow (m^3/s)	0.66	0.17	0.09	0.93
Contribution	71%	19%	10%	100%

Median Flow (cfs)	12.4	3.6	1.8	-
Max Flow (cfs)	1,295	224	435	1,504
Min Flow (cfs)	0.3	0.2	0.1	0.7
Std. Deviation	44.5	9.0	5.5	55.4
Coeff. of Variation	1.91	1.48	1.66	1.69

2.3.1.5 Summary of Flow Characteristics

- Flow Dominance: The analysis confirms that Crooked Lake Ditch is the primary driver of hydrology, delivering nearly three-quarters of the total average inflow to the system. Its influence is most pronounced during storm events, where it produces extreme flood peaks.
- High Variability: All tributaries are classified as "flashy" or "very variable," with Coefficients of Variation (CV) well above 1.0. This indicates that the flow regime is characterized by short-duration, high-magnitude peaks followed by long periods of low baseflow. This is typical of streams in agricultural watersheds with extensive drainage.
- Skewed Distribution: For all inflows, the median flow is significantly lower than the mean flow, indicating a positively skewed distribution. This confirms that the average flow is heavily influenced by a relatively small number of high-flow storm and snowmelt events.
- Extreme Events: The system is subject to extreme event-driven flows. The maximum recorded combined inflow (1,504 cfs) is over 2,000 times greater than the combined minimum baseflow (0.7 cfs), highlighting the dynamic range the lake system must accommodate.

These flow characteristics have direct implications for lake management, influencing everything from water level stability and outlet capacity requirements to the timing and magnitude of nutrient and sediment loading.

For the sake of brevity, all subsequent figures showing boundary condition time-series will display the data for Crooked Lake Ditch (inflow to Branch 2), as it is the dominant tributary with the highest flows and loadings. Data for other tributaries will be shown only if they differ significantly.

2.3.2 Temperature

Water temperature is a primary driver in the CE-QUAL-W2 model due to its influence on nearly all physical and biogeochemical processes. Accurately representing temperature is essential for both hydrodynamic calibration and water quality simulation. Key processes controlled by temperature include:

Density & Stratification: Small changes in temperature directly control water density, which governs the setup and breakdown of thermal stratification.

Heat Exchange: Surface heat exchange with the atmosphere is a primary function of the water-air temperature difference.

Reaction Kinetics: The rates of virtually all chemical and biological reactions, such as nutrient cycling and organic matter decay, are moderated by temperature.

Biological Activity: Algal growth, respiration, and mortality rates are all temperature-dependent.

2.3.2.1 Boundary and Initial Temperature Conditions

Tributary Temperatures: The water temperature for all tributary inflows was defined using a single sub-daily time-series derived from the HSPF watershed model output (Figure 9). Since continuous observed temperature data was not available for each individual tributary, a single representative time-series was applied to all inflows. This is a common simplification, as air temperature is the dominant factor controlling stream temperatures in a relatively compact geographical area.

Initial Conditions: The initial temperature profile for the entire lake on January 1, 2012, was set based on typical late-winter inverse stratification conditions, using historical profile data from the MPCA as a guide.

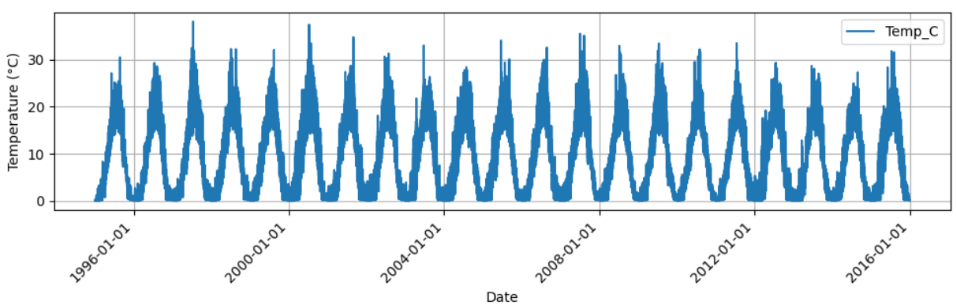

Figure 9. Tributary Inflow Water Temperature Time-Series, 1996-2015.

2.3.3 Water Quality

The primary water quality constituents simulated in the Lake Osakis model were chosen to represent the key eutrophication processes: nutrient cycling, organic matter dynamics, sediment transport, and algal growth.

2.3.3.1 Water Quality Boundary Conditions

Commented [SK1]: Subheading?

Sub-daily loads of nutrients, sediment, and organic matter from all tributaries were derived from the HSPF watershed model output. The specific state variables and their derivation are summarized in Table 5 below.

Table 5. Lake Osakis water quality parameters - boundary conditions.

Parameter	Description	Derivation from HSPF Output
ISS	Inorganic Suspended Solids	Directly derived from the HSPF Total Suspended Solids (TSS) load, assuming a 30/70 fixed organic/inorganic fraction.
Algae	Simulates phytoplankton biomass.	Directly derived from the HSPF algal load.
PO4	Bioavailable Phosphorus (Orthophosphate)	HSPF-simulated load. Phosphorus serves as the primary limiting nutrient for phytoplankton growth in the model.
NHx	Ammonium	HSPF-simulated load.
NOx	**Nitrate-Nitrite**	**HSPF-simulated load**
LDOM/LPOM	Labile Dissolved/Particulate Organic Matter	Derived from several HSPF organic and inorganic loads, described below.
RDOM/RPOM	Refractory Dissolved/Particulate Organic Matter	Derived from several HSPF organic and inorganic loads, described below.
TDS	Total Dissolved Solids	Based on typical regional values and calibrated.
DO	Dissolved Oxygen	Assumed to be at or near saturation, based on tributary temperature.

Inorganic Suspended Solids (ISS): Given the concern over material loading from JD2, ISS is a key state variable (Figure 10). It is the primary driver of turbidity in the model, which controls light penetration through the water column and can limit algal growth, directly impacting water clarity. ISS was derived from the HSPF Total Suspended Solids (TSS) load, as described in the organic matter derivation below.

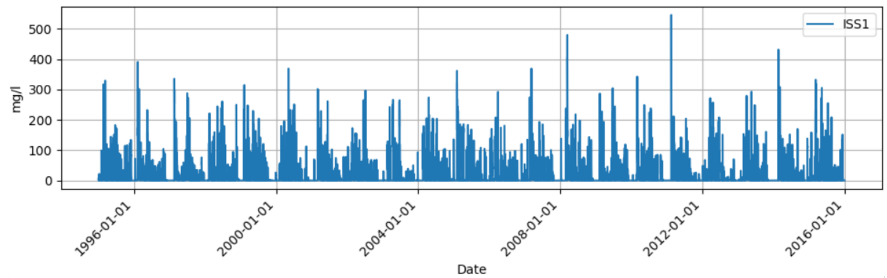

Figure 10. Inorganic Suspended Solids (ISS) concentration time-series for branch 2.

Bioavailable Phosphorus (PO_4): Phosphorus serves as the primary nutrient for phytoplankton growth, and in many freshwater systems like Lake Osakis, it is considered the limiting nutrient for algal biomass. In the model, phosphorus is assumed to be completely available as orthophosphate (PO_4) for uptake by phytoplankton. The tributary PO_4 load was dynamically calculated by HSPF based on watershed processes (Figure 11).

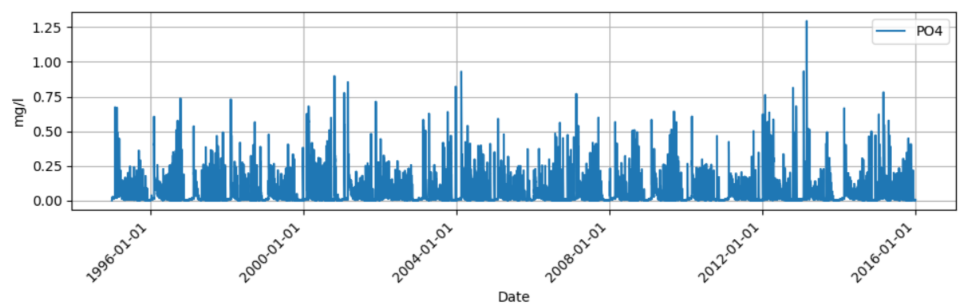

Figure 11. Bioavailable Phosphorus (PO_4) concentration time-series for branch 2.

Nitrogen (NHx and NOx): Nitrogen is another essential nutrient for algae. The model simulates two forms: ammonium (NH_4) (Figure 12), which is preferentially taken up by algae, and nitrate-nitrite (NOx) (Figure 13). Both were derived from HSPF output.

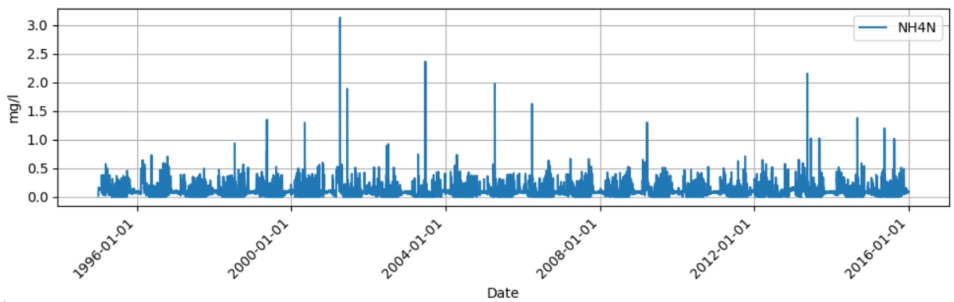

Figure 12. Ammonium (NH_4) concentration time-series for branch 2.

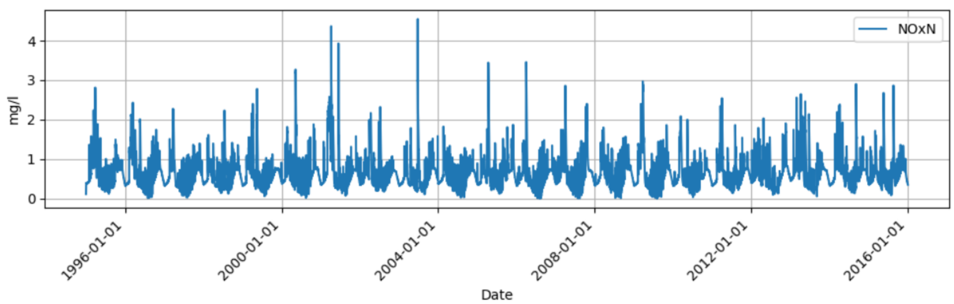

Figure 13. Nitrate-nitrite (NOx) concentration time-series for branch 2.

Algae: Algal biomass, measured as Chlorophyll-a, represents the base of the lake's food web and is the primary indicator of eutrophic conditions. For this study, it is simulated as five representative groups to capture the overall phytoplankton response to nutrient loads. Total tributary algal concentrations were provided from HSPF output (Figure 14) and divided into five algal groups.

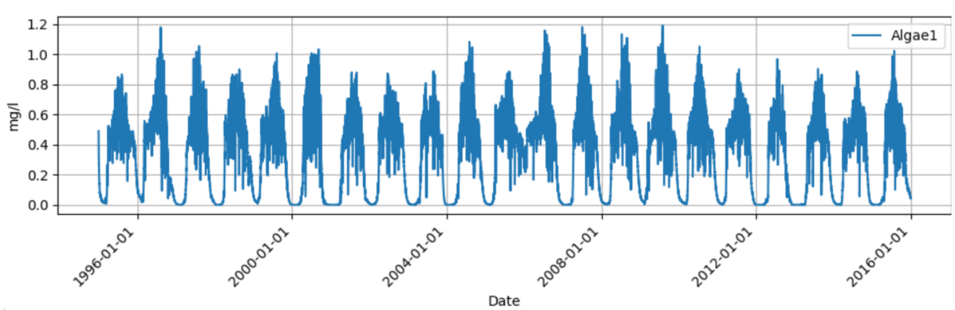

Figure 14. Algal Biomass concentration time-series for branch 2.

Dissolved Oxygen (DO): DO is crucial for aquatic life and mediates key chemical processes, including the release of phosphorus from bottom sediments. Tributary DO concentrations were assumed to be at or near saturation, calculated based on the incoming water temperature and provided by HSPF (Figure 15).

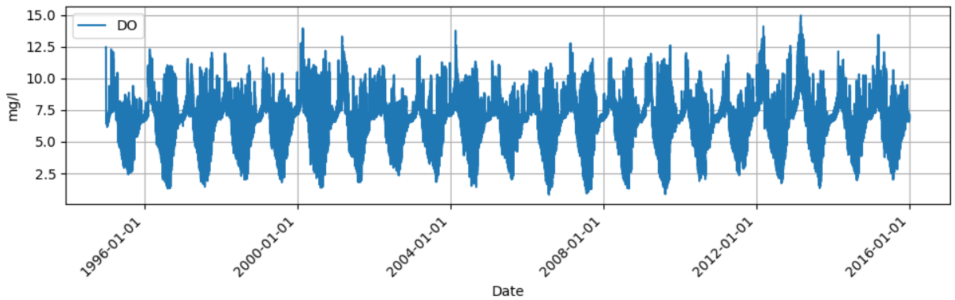

Figure 15. Dissolved Oxygen (DO) concentration time-series for branch 2.

Organic Matter: The decay of organic matter is a critical process, serving as an internal source of nutrients and a primary sink for dissolved oxygen. Organic matter enters the lake via allochthonous sources (produced outside the system and delivered by tributaries) and autochthonous sources (produced within the lake, primarily by phytoplankton).

As direct, continuous measurements of organic matter fractions are not available for the tributaries, the four required state variables—labile dissolved organic matter (LDOM) (Figure 16), refractory dissolved organic matter (RDOM)(Figure 17), labile particulate organic matter (LPOM)(Figure 18), and refractory particulate organic matter (RPOM)(Figure 19)—were estimated from the HSPF model's time-series outputs for Total Organic Carbon (TOC) and Total Suspended Solids (TSS).

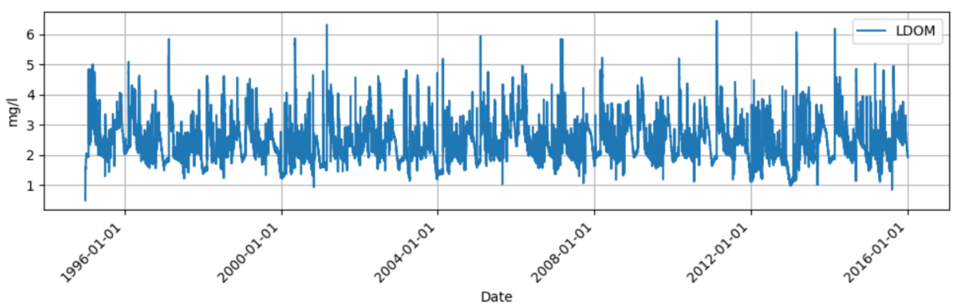

Figure 16. LDOM concentration time-series for branch 2.

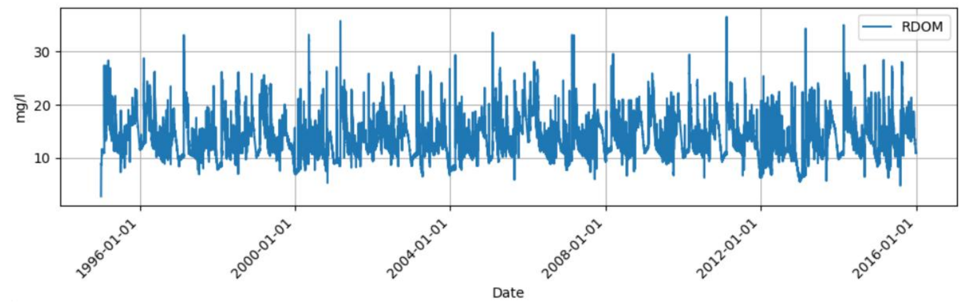

Figure 17. RDOM concentration time-series for branch 2.

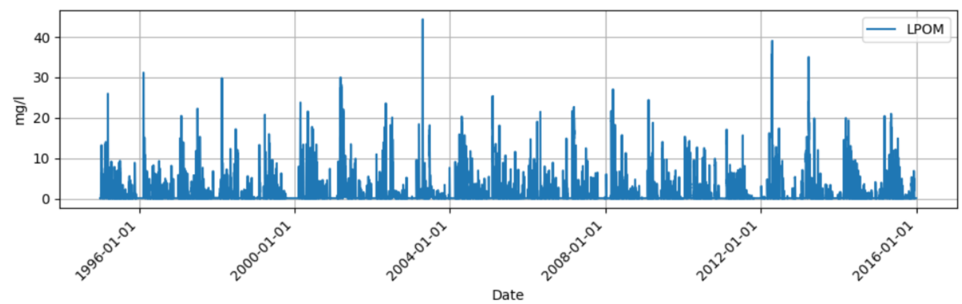

Figure 18. LPOM concentration time-series for branch 2.

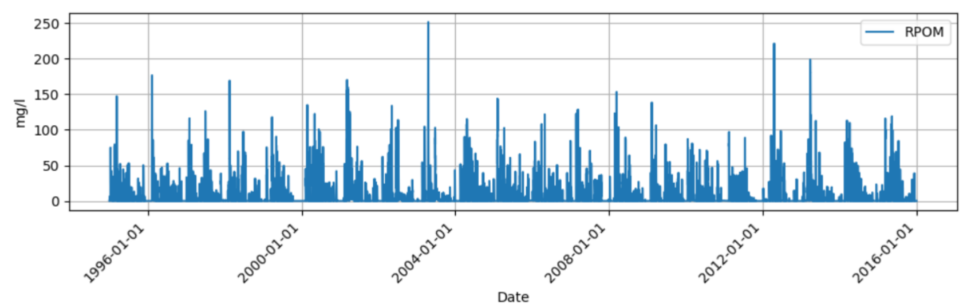

Figure 19. RPOM concentration time-series for branch 2.

2.3.3.2 Derivation of Organic Matter and ISS Fractions

The methodology to convert the HSPF outputs into CE-QUAL-W2 inputs is detailed below.

Commented [SK2]: Subheading?

1. Foundational Assumptions:
A set of literature-based assumptions were established to guide the fractionation of lumped water quality parameters (Chapra 1997):

- TSS Partitioning: Incoming TSS was assumed to be 70% inorganic (ISS) and 30% volatile/organic (VSS/POM), which is typical for a clay/silt dominated agricultural watershed.
- TOC Partitioning: The TOC load was assumed to be 90% dissolved (DOC) and 10% particulate (POC).
- Labile vs. Refractory Split: Both dissolved and particulate organic matter pools were split into a 15% labile (fast-decaying) fraction and an 85% refractory (slow-decaying) fraction.
- Carbon to Organic Matter Conversion: A stoichiometric ratio (δ_c) of 0.45 g C / g OM was used to convert carbon mass to total organic matter mass (OM = C / 0.45). This results in a conversion factor of 2.22 (OM = C × 2.22).

2. Calculation Steps:
The tributary concentrations for each W2 variable were then calculated as follows:

- Inorganic Solids:
  ISS (mg/L) = TSS * 0.70
- Dissolved Organic Matter (DOM):
  LDOM (mg/L) = TOC * 0.90 * 0.15 * 2.22
  RDOM (mg/L) = TOC * 0.90 * 0.85 * 2.22
- Particulate Organic Matter (POM): The POM load was derived from the organic portion of the TSS, ensuring the contribution from tributary algae (simulated by HSPF) was subtracted to prevent double-counting.
  POM_total (mg/L) = (TSS * 0.30) - Algal_OM
  LPOM (mg/L) = POM_total * 0.15
  RPOM (mg/L) = POM_total * 0.85

This approach ensures that the highly variable sediment events from the TSS signal are represented as POM loads, while the smoother seasonal patterns from the TOC signal define the DOM loads. All final concentrations were expressed in mg/L as organic matter for direct use in the CE-QUAL-W2 model.

2.3.4 Meteorological Data

Input files of the meteorological forcing in the appropriate units and format were prepared using hourly air temperature (Figure 20), dew point temperature (Figure 21), wind speed (Figure 22), wind direction (Figure 23), cloud cover and solar radiation (Figure 24) reported from KAXN weather station, located about 10 miles west of Lake Osakis at the Chandler Field Airport in Alexandria, Minnesota.

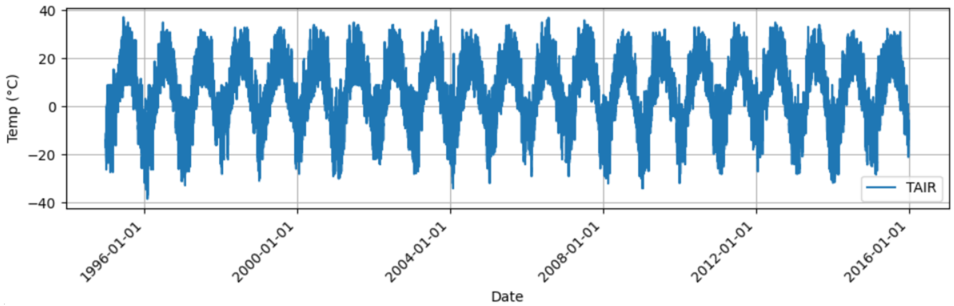

Figure 20. Hourly Air Temperature from KAXN Weather Station, 1996-2015.

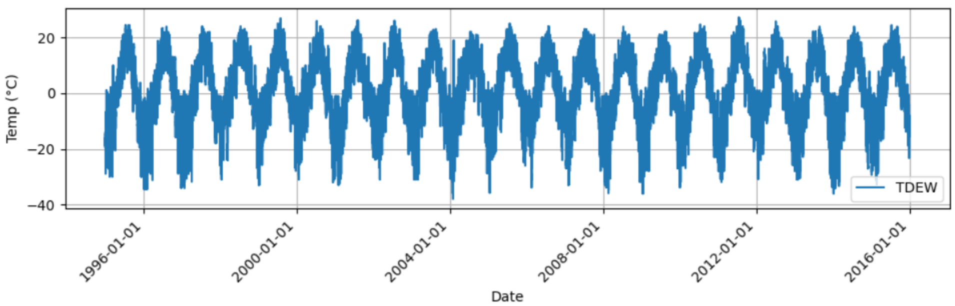

Figure 21. Hourly Dew Point Temperature from KAXN Weather Station, 1996-2015.

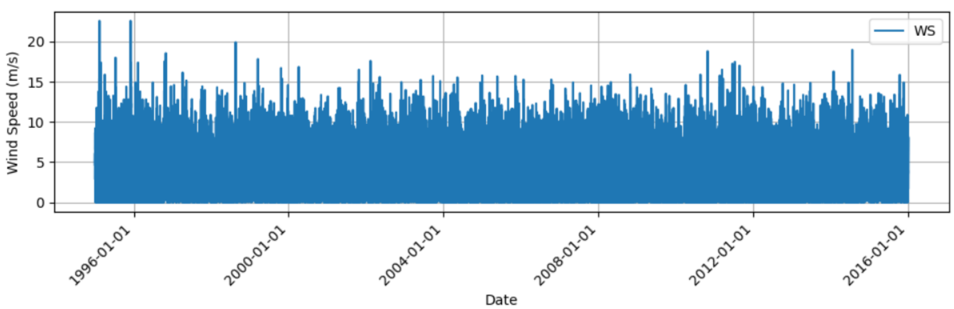

Figure 22. Hourly Wind Speed from KAXN Weather Station, 1996-2015.

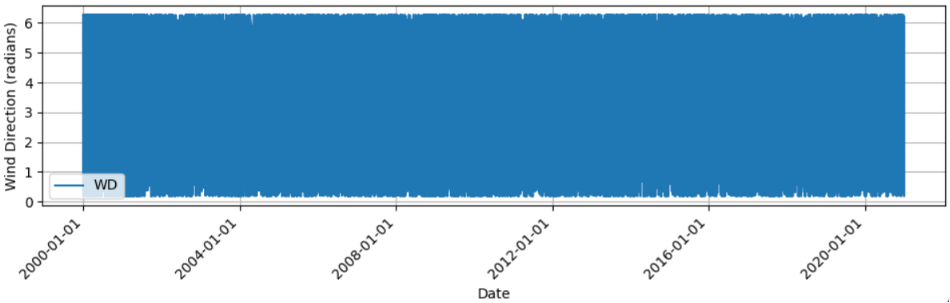

Figure 23. Hourly Wind Direction from KAXN Weather Station, 1996-2015.

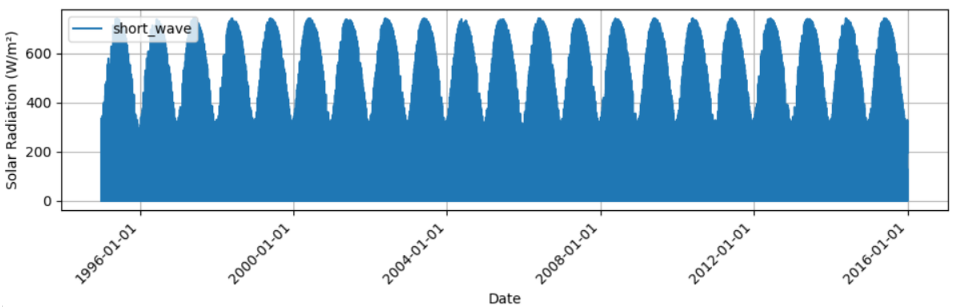

Figure 24. Hourly Solar Radiation from KAXN Weather Station, 1996-2015.

3 CE-QUAL-W2 Model Performance

3.1 Model Calibration

The Lake Osakis CE-QUAL-W2 model was calibrated using a robust, multi-faceted approach to ensure its predictive accuracy for evaluating water quality improvement scenarios. The core strategy was to use comprehensive monitoring data from 2012 to develop a single, optimized set of hydraulic and water quality parameters, with the goal of minimizing the statistical difference between simulated results and observed data for the primary open-water season (May-October).

To efficiently evaluate thousands of potential parameter combinations, the calibration process was automated using a custom Python script leveraging the SPOTPY optimization package. This script employed the Shuffled Complex Evolution (SCE-UA) algorithm (Duan et al., 1992) to systematically find the parameter set that produced the lowest statistical error when compared to observed values. The calibration focused on a "weight of evidence" approach, where goodness-of-fit statistics (Nash-Sutcliffe Efficiency, Root Mean Square Error, etc.) were used to guide adjustments while also ensuring the model could reproduce key ecological phenomena, such as algal bloom succession and the development of anoxia.

The primary source for observational data was the Minnesota Pollution Control Agency's (MPCA) Environmental Quality Information System (EQuIS) database. The modeling process was split into distinct calibration and validation phases:

Calibration (2012): The model was formally calibrated against observed data from the 2012 open-water season. This year was selected due to the availability of comprehensive, concurrent data from two distinct monitoring stations (Figure 25), which allowed for a robust spatial calibration:

Four Mile Hole (Site ID: 21-0130-00-209): The primary, deep-water station.

Lindberg's Resort (Site ID: 21-0130-00-203): A secondary, shallower station.

Validation (1996-2015): The calibrated parameter set was then validated across the entire 1996-2015 simulation period using the full historical dataset from all three primary monitoring stations (including Site ID: 21-0130-00-102).

Table 6 summarizes the observational dataset used for the 2012 calibration, detailing the parameters, collection frequency, and specific calibration purpose for each.

Table 6. Observational data available from the EQuIS database

Parameter	Site(s)	Collection Method / Frequency	Calibration Purpose
Temperature & Dissolved Oxygen	209, 203	Depth profiles collected approximately monthly.	Hydrodynamic calibration; simulating thermal stratification and the rate/extent of hypolimnetic anoxia.
Chlorophyll-a	209, 203	Surface (epilimnion) grab samples collected monthly.	Nutrient and algal dynamics; calibrating algal growth, settling, and internal phosphorus loading.
Nutrient Species (PO_4, NOx)	209, 203	Surface and hypolimnion samples, typically spring and late summer.	Nutrient cycling calibration; ensuring correct simulation of nutrient uptake by algae and release from sediments.

This comprehensive dataset provided the necessary information to rigorously calibrate the model's simulation of the key eutrophication processes occurring in Lake Osakis, as documented in the nutrient TMDL study (MPCA, 2023).

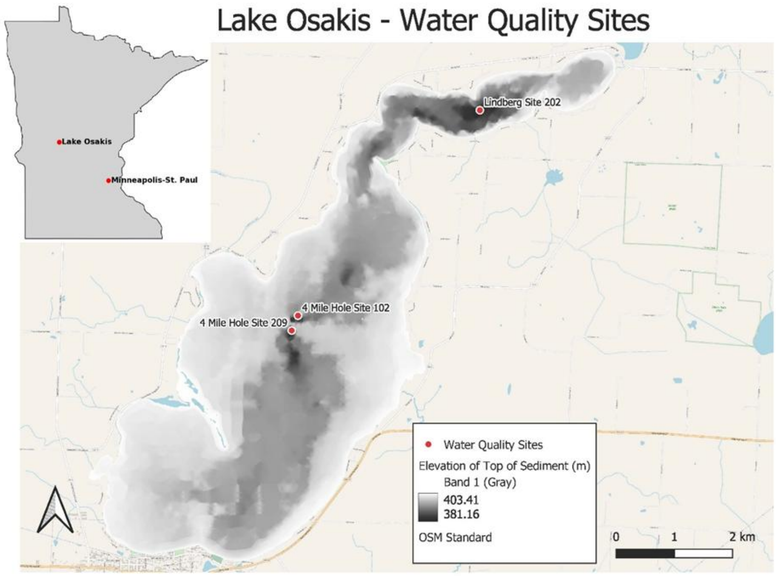

Figure 25. Location of MPCA Water Quality Monitoring Sites.

3.2 Model Calibration / Validation Approach

3.2.1 Performance Metrics

Model performance was evaluated using a dual approach combining visual diagnostics and quantitative statistics. Graphical assessments included direct comparisons of observed versus simulated time-series and vertical profile plots. Quantitative performance was characterized using three primary statistical metrics: Mean Absolute Error (MAE), Root Mean Square Error (RMSE), and the Nash–Sutcliffe Efficiency (NSE)—a widely accepted metric for evaluating the predictive power of environmental models.

3.2.2 Calibration Targets

Table 7 lists the target calibration goals for the primary and secondary state variables, expressed as the desired maximum Mean Absolute Error (MAE). These targets are based on standard professional practice for models of this complexity.

Table 7. Calibration Targets

Variable	Target AME
Primary Calibration Variables	
Temperature	< 1.0 °C
Dissolved Oxygen	< 2.0 mg/L
Total Phosphorus	< 0.02 mg/L
Orthophosphate (PO_4)	< 0.01 mg/L
Secondary Calibration Variables	
Chlorophyll a	< 10.0 µg/L
Total Kjeldahl Nitrogen	< 0.4 mg/L
Ammonium (NH_4)	< 0.06 mg/L
Nitrate + Nitrite (NOx)	< 0.1 mg/L

Commented [SK3]: Ammonia is NH3, Ammonium is NH4. Im assuming this should be Ammonium since ammonia is a gas.

3.2.3 Hydrodynamic Calibration: Water Balance

The first and most fundamental step in model calibration is achieving an accurate water balance. This ensures that the total volume of water entering, leaving, and being stored in the model is consistent with observations. The model's water balance was calibrated by comparing the simulated lake surface elevation to observed lake level data provided by the Sauk River Watershed District (SRWD).

3.2.3.1 Initial Model Run (Before)

The initial model run used only the three primary gauged tributaries (Crooked Lake Ditch, North Branch, and Boss Creek East) as inputs. As shown in the "before" Figure 26, this configuration resulted in a significant underestimation of lake levels. The simulated water surface elevation (orange line) consistently fell below the observed data (blue line), with the discrepancy increasing over time. This indicates that the gaged tributary inflows alone were not sufficient to account for all the water entering the lake. The model was clearly missing a substantial source of water.

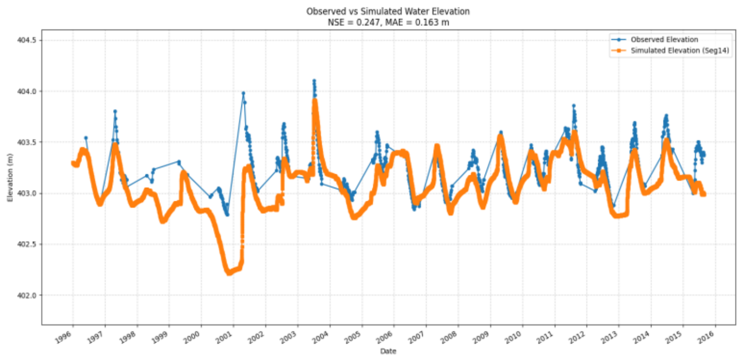

Figure 26. Water Surface Elevation Comparison before adding Distributed Tributary.

3.2.3.2 Water Balance Correction: Distributed Tributary

To correct this water balance deficit, an ungaged or "distributed" tributary was added to the model. This inflow represents the cumulative contribution of runoff from the land area draining directly to the lake, groundwater inputs, and any minor ungaged streams that were not explicitly included in the HSPF model.

A new inflow time-series was generated using a water balance script, which calculated the daily flow required to make the simulated lake elevations match the observed data. This calculated inflow shown in Figure 27 represents the "missing" water from the system.

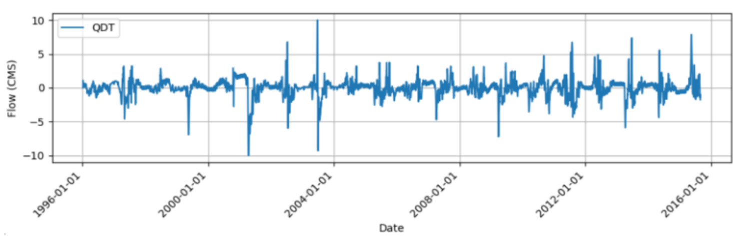

Figure 27. Distributed Tributary Flow Time-Series.

.

3.2.3.3 Final Model Run (After)

The "after" Figure 28 demonstrates the model's performance with the inclusion of the calculated distributed tributary flow. The result is an excellent match between the simulated (orange line) and observed (blue line) water surface elevations throughout the multi-year simulation period. The model now accurately captures both the seasonal fluctuations and the long-term trends in lake level.

This successful water balance calibration provides a robust foundation for the subsequent calibration of temperature and water quality, ensuring that hydrodynamic transport and residence times are simulated correctly.

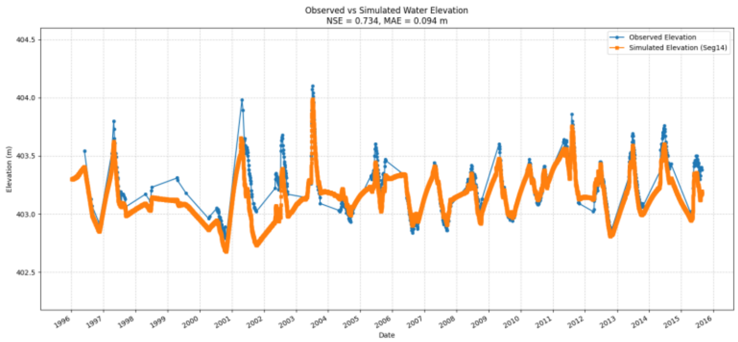

Figure 28. Model Comparison to Observed Water Level Measurements after adding Distributed Tributary.

3.2.4 Model Calibration Parameters

The calibration of the Lake Osakis CE-QUAL-W2 model was an iterative process designed to systematically adjust physical and biogeochemical coefficients to match observed data from the 2012 open-water season. This process revealed key ecological dynamics within the lake and established a robust, stable framework for simulating water quality.

3.2.4.1 Sediment Parameterization and Stability

Rather than adjusting active hydrodynamic coefficients, the initial phase of physical calibration focused on sediment transport behavior and numerical stability. While testing the model's response to sediment resuspension parameters, enabling the active resuspension algorithm (SEDRC = ON) introduced severe numerical instability and generated highly unrealistic concentrations of suspended solids in the lower layers of the water column.

To stabilize the simulation, sediment resuspension was deactivated (SEDRC = OFF). This adjustment successfully stabilized the model and indicated that, within the Lake Osakis system, suspended sediment dynamics are primarily dominated by the transport and settling of external tributary loads rather than internal resuspension.

3.2.4.2 Calibrating Oxygen and Nutrient Cycle

The primary biogeochemical calibration challenge was resolving the model's initial inability to reproduce the high summer dissolved oxygen (DO) supersaturation levels (exceeding 120%) observed in the lake's surface waters. This discrepancy pointed to an imbalance in the tightly coupled nutrient-algae-oxygen cycle, prompting two competing hypotheses: either the simulated algal growth was too low to generate sufficient oxygen, or the oxygen sinks stemming from organic matter decay were excessively high.

A systematic sensitivity analysis revealed that both processes required adjustment. To match observed surface DO without causing runaway algal blooms, a balanced tuning approach was applied. This involved moderately increasing the maximum algal growth rate (AG) while simultaneously reducing both the algal mortality rate (AM) and the organic matter decay rates (specifically LDOMDK and LPOMDK). This coordinated adjustment successfully simulated the observed summer oxygen peaks while preventing a rapid organic decay "short-circuit" in the surface waters.

3.2.4.3 Justification for a Five-Algal-Group Structure

Following the primary nutrient calibration, a secondary issue emerged where the model simulated an unrealistic algal bloom in the dark, bottom waters (an artificial deep chlorophyll maximum). This artifact was identified as a known limitation of utilizing a single, generalized algal group. A single biological pool relies on a static set of kinetic parameters that cannot simultaneously represent the diverse ecological niches present in Lake Osakis—such as high-light adapted surface species versus shade-tolerant deeper species.

To resolve this limitation and better represent the lake's ecology, the model structure was expanded to feature five distinct functional algal groups: Diatoms, Greens, two separate Cyanobacteria groups, and Flagellates. This multi-group architecture allowed for the assignment of unique, literature-supported kinetic parameters for light, temperature, and nutrient uptake to each group. This structural modification successfully eliminated the artificial deep-water blooms and enabled the model to accurately replicate observed seasonal algal succession and vertical distribution.

3.2.4.4 Parameter Benchmarking

To ensure that all final calibrated coefficients remained physically realistic and ecologically defensible, they were benchmarked against values from other peer-reviewed CE-QUAL-W2 applications on similar Minnesota lakes. Specifically, parameter ranges were compared to the U.S. Geological Survey studies of Madison Lake and Pearl Lake (Smith et al., 2017). Both waterbodies are situated in agricultural watersheds and experience similar eutrophication challenges, making them highly appropriate regional reference points. The final calibrated coefficients for the Lake Osakis model are presented in Tables 8 through 18.

3.2.5 Primary Calibration Coefficients

Table 8. Hydraulic, Light, and Structural Coefficients

ID	Description	Default	Madison	Pearl	Osakis Final
AX	Horizontal eddy viscosity (m^2/s)	1.0	1.0	1.0	1.0
DX	Vertical eddy coefficient (m^2/s)	1.0	1.0	1.0	1.0
CBHE	Sediment heat exchange coeff. ($W/m^2/°C$)	1.16	1.5	1.3	**1.5951**
TSED	Temperature of sediment (°C)	10.0	-	-	10

FI	Interfacial friction factor	0.0	0.015	0.015	**0.015**
TSEDF	Fraction of heat returned to water	1.0	0.75	0.1	1
TYPE	Type of waterbody	LAKE	LAKE	LAKE	Lake
EQN#	Reaeration equation number	1	9	1	**2**
AZC	Vertical turbulence closure algorithm	W2	W2	TKE	W2
BETA	Fraction of surface solar absorption	0.45	0.55	0.45	0.45
EXH2O	Extinction by water (1/m)	0.45	0.25	0.25	**0.25**
EXSS	Extinction by solids (m^2/g)	0.17	0.1	0.2	**0.1**
EXOM	Extinction by organic matter (m^2/g)	0.17	0.1	0.2	**0.2**

Table 9. Spatially-Varied WSC. Values assigned by zone from wsc.csv. Dummy segments are excluded.

Zone	Segments	WSC Value
Upper Lake	2-10	**0.59**
Lower Lake	11-26	**1.45**
Miller Bay	29-32	**1.45**

3.2.6 Algal Community Coefficients

Note: The reference (E. K. Smith 2014) studies modeled four algal groups. The Osakis model uses five, including two distinct cyanobacteria groups, one of which is modeled as buoyant.

Table 10. Diatoms (ALG1) Coefficients

ID	Description	Default	Madison	Pearl	Osakis Final
AG	Max growth rate	1.5	3.82	1.38	**2.0**

AR	Respiration rate	0.1	0.02	0.04	**0.02**
AE	Excretion rate	0.05	0.02	0.025	**0.02**
AM	Mortality rate	0.1	0.06	0.07	**0.15**
AS	Settling rate	0.1	0.2	0.15	**0.7**
AHSP	P Half-saturation	0.002	0.0065	0.004	**0.005**
AHSN	N Half-saturation	0.01	0.025	0.01	**0.02**
AHSSI	Si Half-saturation	0.0	0	0	0
ASAT	Light saturation	30.0	150	30	**125**
AT1	Lower temp for growth	4.0	5	5	**5**
AT2	Lower temp for max growth	8.0	13	14	**12**
AT3	Upper temp for max growth	20.0	18	23	**18**
AT4	Upper temp for growth	25.0	21	27	**22**
AK1	Fraction growth at AT1	0.1	0.1	0.1	0.1
AK2	Fraction growth at AT2	0.99	0.99	0.99	0.99
AK3	Fraction growth at AT3	0.99	0.99	0.9	0.99
AK4	Fraction growth at AT4	0.1	0.1	0.1	0.1
ALGP	Algal P stoichiometry	0.005	0.0045	0.0041	**0.0045**
ALGN	Algal N stoichiometry	0.08	0.085	0.0795	**0.085**

ALGC	Algal C stoichiometry	0.45	0.45	0.45	0.45
ALGSI	Algal Si stoichiometry	0.18	0.18	0.18	**0.0**
ACHLA	Biomass:Chl-a ratio	50.0	0.09	0.1	**0.09**
ALPOM	Fraction algal death to POM	0.7	0.85	0.75	**0.8**
ANEQN	NH4 preference equation #	2	1	2	**1**
ANPR	NH4 preference half-saturation	0.01	0.02	0.02	**0.02**
O2AR	O2 stoich. for algal respiration	1.4	1.1	1.1	**1.1**
O2AG	O2 stoich. for algal growth	1.4	1.65	1.4	**1.65**

Table 11. Greens (ALG2) Coefficients

ID	Description	Default	Madison	Pearl	Osakis Final
AG	Max growth rate	1.5	2.1	1.21	**2**
AR	Respiration rate	0.1	0.04	0.04	**0.04**
AE	Excretion rate	0.05	0.05	0.025	0.05
AM	Mortality rate	0.1	0.09	0.07	**0.12**
AS	Settling rate	0.1	0.12	0.1	**0.12**
AHSP	P Half-saturation	0.002	0.0065	0.004	**0.0065**
AHSN	N Half-saturation	0.01	0.03	0.014	**0.03**
ASAT	Light saturation	30.0	50	45	**80**

AT1	Lower temp for growth	4.0	10	10	**10**
AT2	Lower temp for max growth	8.0	22	18	**22**
AT3	Upper temp for max growth	20.0	28	25	**28**
AT4	Upper temp for growth	25.0	32	30	**32**
AK1	Fraction growth at AT1	0.1	0.005	0.1	**0.005**
AK2	Fraction growth at AT2	0.99	0.65	0.99	**0.65**
AK3	Fraction growth at AT3	0.99	0.99	0.99	0.99
AK4	Fraction growth at AT4	0.1	0.1	0.1	0.1
ALGP	Algal P stoichiometry	0.005	0.0085	0.0036	**0.0085**
ALGN	Algal N stoichiometry	0.08	0.085	0.0825	**0.085**
ALGC	Algal C stoichiometry	0.45	0.45	0.45	0.45
ACHLA	Biomass:Chl-a ratio	50.0	0.1	0.15	**0.1**
ALPOM	Fraction algal death to POM	0.7	0.7	0.75	0.7
ANEQN	NH4 preference equation #	2	1	2	**1**
ANPR	NH4 preference half-saturation	0.01	0.02	0.02	**0.02**

O2AR	O2 stoich. for algal respiration	1.4	1.1	1.1	**1.1**
O2AG	O2 stoich. for algal growth	1.4	1.4	1.4	1.4

Table 12. Cyanobacteria 1 (ALG3) Coefficients

ID	**Description**	**Default**	**Madison**	**Pearl**	**Osakis Final**
AG	Max growth rate	1.5	1.62	1.38	**2.00**
AR	Respiration rate	0.1	0.04	0.04	**0.04**
AE	Excretion rate	0.05	0.07	0.025	**0.07**
AM	Mortality rate	0.1	0.08	0.12	**0.15**
AS	Settling rate	0.1	0.08	0.1	**.08**
AHSP	P Half-saturation	0.002	0.0062	0.0045	**0.0062**
AHSN	N Half-saturation	0.01	0.002	0.002	**0.002**
ASAT	Light saturation	30.0	60	120	**100**
AT1	Lower temp for growth	4.0	13	11	**13**
AT2	Lower temp for max growth	8.0	20	17	**20**
AT3	Upper temp for max growth	20.0	32	28	**32**
AT4	Upper temp for growth	25.0	35	35	**35**
AK1	Fraction growth at AT1	0.1	0.01	0.3	**0.01**
AK2	Fraction growth at AT2	0.99	0.99	0.95	0.99

AK3	Fraction growth at AT3	0.99	0.99	0.85	0.99
AK4	Fraction growth at AT4	0.1	0.1	0.1	0.1
ALGP	Algal P stoichiometry	0.005	0.0075	0.0049	**0.0075**
ALGN	Algal N stoichiometry	0.08	0.08	0.0655	0.08
ALGC	Algal C stoichiometry	0.45	0.45	0.45	0.45
ACHLA	Biomass:Chl-a ratio	50.0	0.06	0.15	**0.06**
ALPOM	Fraction algal death to POM	0.7	0.7	0.75	0.7
ANEQN	NH4 preference equation #	2	1	2	**1**
ANPR	NH4 preference half-saturation	0.01	0.02	0.02	**0.02**
O2AR	O2 stoich. for algal respiration	1.4	0.95	1.1	**.95**
O2AG	O2 stoich. for algal growth	1.4	1.1	2.4	**1.1**

Table 13. Cyanobacteria 2 (buoyant, ALG4) Coefficients

ID	Description	Default	Madison	Pearl	Osakis Final
AG	Max growth rate	1.5	1.62	1.38	**2.0**
AR	Respiration rate	0.1	0.04	0.04	**.08**
AE	Excretion rate	0.05	0.07	0.025	**.04**
AM	Mortality rate	0.1	0.08	0.12	**.16**
AS	Settling rate	0.1	0.08	0.1	**Buoyant**

AHSP	P Half-saturation	0.002	0.0062	0.0045	**.0005**
AHSN	N Half-saturation	0.01	0.002	0.002	.01
ASAT	Light saturation	30.0	60	120	**225**
AT1	Lower temp for growth	4.0	13	11	**18**
AT2	Lower temp for max growth	8.0	20	17	**22**
AT3	Upper temp for max growth	20.0	32	28	**32**
AT4	Upper temp for growth	25.0	35	35	**35**
AK1	Fraction growth at AT1	0.1	0.01	0.3	.1
AK2	Fraction growth at AT2	0.99	0.99	0.95	.99
AK3	Fraction growth at AT3	0.99	0.99	0.85	.99
AK4	Fraction growth at AT4	0.1	0.1	0.1	.1
ALGP	Algal P stoichiometry	0.005	0.0075	0.0049	**.006**
ALGN	Algal N stoichiometry	0.08	0.08	0.0655	**.11**
ALGC	Algal C stoichiometry	0.45	0.45	0.45	.45
ACHLA	Biomass:Chl-a ratio	50.0	0.06	0.15	**.05**
ALPOM	Fraction algal death to POM	0.7	0.7	0.75	**.8**
ANEQN	NH4 preference equation #	2	1	2	**1**

ANPR	NH4 preference half-saturation	0.01	0.02	0.02	**.02**
O2AR	O2 stoich. for algal respiration	1.4	0.95	1.1	**1.1**
O2AG	O2 stoich. for algal growth	1.4	1.1	2.4	1.4

Table 14. Flagellates (ALG5) Coefficients

ID	Description	Default	Madison	Pearl	Osakis Final
AG	Max growth rate	1.5	2.12	1.52	**2.12**
AR	Respiration rate	0.1	0.04	0.04	**.04**
AE	Excretion rate	0.05	0.04	0.025	**.04**
AM	Mortality rate	0.1	0.09	0.07	**.12**
AS	Settling rate	0.1	0.1	0.1	.1
AHSP	P Half-saturation	0.002	0.0065	0.004	**.0065**
AHSN	N Half-saturation	0.01	0.03	0.01	**.03**
ASAT	Light saturation	30.0	20	30	**20**
AT1	Lower temp for growth	4.0	14	6	**14**
AT2	Lower temp for max growth	8.0	24	16	**24**
AT3	Upper temp for max growth	20.0	28	24	**28**
AT4	Upper temp for growth	25.0	30	29	**30**
AK1	Fraction growth at AT1	0.1	0.005	0.1	**.005**

AK2	Fraction growth at AT2	0.99	0.88	0.94	**.88**
AK3	Fraction growth at AT3	0.99	0.99	0.64	.99
AK4	Fraction growth at AT4	0.1	0.1	0.1	.1
ALGP	Algal P stoichiometry	0.005	0.006	0.0037	**.006**
ALGN	Algal N stoichiometry	0.08	0.085	0.085	**.085**
ALGC	Algal C stoichiometry	0.45	0.45	0.45	.45
ACHLA	Biomass:Chl-a ratio	50.0	0.1	0.1	**.1**
ALPOM	Fraction algal death to POM	0.7	0.7	0.75	.7
ANEQN	NH4 preference equation #	2	1	2	**1**
ANPR	NH4 preference half-saturation	0.01	0.02	0.02	**.02**
O2AR	O2 stoich. for algal respiration	1.4	1.25	1.1	**1.25**
O2AG	O2 stoich. for algal growth	1.4	1.4	1.4	1.4

Table 15. Organic Matter Coefficients

ID	Description	Default	Madison	Pearl	Osakis Final
LDOMDK	Labile DOM decay (1/day)	0.01	0.0725	0.1	**0.06**
RDOMDK	Refractory DOM decay (1/day)	0.001	0.002	0.001	**0.002**

LRDDK	Labile-to-refractory DOM decay (1/day)	0.01	0.02	0.01	0.01
LPOMDK	Labile POM decay (1/day)	0.1	0.05	0.08	0.1
RPOMDK	Refractory POM decay (1/day)	0.005	0.002	0.001	**0.002**
LRPDK	Labile-to-refractory POM decay (1/day)	0.01	0.02	0.01	0.01
POMS	POM settling rate (m/day)	0.1	0.125	0.125	**1.0**
ORGP	OM P stoichiometry	0.0025	0.0065	0.0025	**0.005**
ORGN	OM N stoichiometry	0.07	0.095	0.105	**0.08**
ORGC	OM C stoichiometry	0.45	0.45	0.45	0.45
ORGSI	OM Si stoichiometry	0.18	0.18	0.18	0.18
O2OM	O2 stoichiometry for OM decay	1.4	1.4	1.4	1.4
OMT1	Lower temp for OM decay (°C)	4.0	5	4	**5**
OMT2	Upper temp for OM decay (°C)	25.0	25	25	**30**
OMK1	Fraction OM decay at OMT1	0.1	0.1	0.1	0.1
OMK2	Fraction OM decay at OMT2	0.99	0.99	0.99	0.99

Table 16. Nutrient Coefficients

ID	Description	Default	Madison	Pearl	Osakis Final
PO4R	P sediment release ($g/m^2/day$)	0.0	0.012	0.0025	**0.005**
PARTP	P partitioning coefficient	0.0	0	0	0
NH4R	NH4 sediment release ($g/m^2/day$)	0.0	0.004	0.0	0.000
NH4DK	Nitrification rate (1/day)	0.08	0.095	0.2	**0.05**
NO3DK	Denitrification rate (1/day)	0.02	0.0575	0.16	**0.10**
NO3S	Denitrification from sediments (m/day)	0.0	0.003	0.15	**0.05**
DSIR	Si sediment release (frac. of SOD)	0.0	0.1	0.1	**0.1**
PSIS	Particulate biogenic silica settling (m/day)	1.0	1.0	1.0	1
PSIDK	Particulate biogenic silica decay (1/day)	0.3	0.3	0.3	0.3
O2LIM	DO half-saturation constant (g/m^3)	0.5	0.1	0.7	**0.1**

Values assigned by zone from w2_con.csv. Dummy segments are excluded.

Table 17. Spatially-Varied Sediment Oxygen Demand (SOD). Values assigned by zone from w2_con.csv. Dummy segments are excluded.

Zone	Segments	SOD Value ($g/m^2/day$)
Upper Lake	2-10	**2**

Lower Lake	11-26	**1.5**
Miller Bay	29-32	**1.5**

Table 18. Sediment Transport Coefficients

ID	Description	Default	Madison	Pearl	Osakis Final
SEDK	First-order sediment decay (1/day)	0.0	0.04	0.1	**0.08**
SSS	Settling velocity, solids (m/day)	1.0	1.0	1.0	**0.1**
SEDRC	Resuspension of solids	ON	-	-	OFF
TAUCR	Critical shear for resuspension (dyne/cm²)	0.1	0.05	0.05	**1.5**

3.2.7 Water Temperature and Dissolved Oxygen

The model's hydrodynamic calibration focused on accurately reproducing the lake's thermal structure, which is the primary driver of its physical and biogeochemical processes. A successful temperature calibration ensures the model correctly simulates the onset, strength, and duration of summer thermal stratification and the timing of seasonal turnover events. These mixing dynamics are critical as they control the vertical transport of heat, nutrients, and dissolved oxygen throughout the water column (Chapra 1997). Key parameters adjusted to achieve this included coefficients for light extinction, wind sheltering, and sediment heat exchange. As shown in the vertical profiles (

Figure *29* and Figure 32) and the continuous time-series data (Figure 30 and Figure 33), the final calibrated model successfully reproduces the seasonal pattern of thermal stratification at both the Four Mile Hole and Lindberg stations, closely matching observed temperature data.

Dissolved Oxygen (DO) is a primary indicator of lake health and was a key focus of the water quality calibration. The model was calibrated to match two critical, opposing processes:

Hypolimnetic Anoxia: The model successfully simulates the decline of DO in the hypolimnion (bottom waters) during summer, leading to anoxia (Figure 31 and Figure 34). This process is correctly driven by the decomposition of organic matter, which consumes oxygen via Sediment Oxygen Demand (SOD). Accurately simulating anoxia is essential, as it is the trigger for the release of phosphorus from lake sediments (Nürnberg 1984).

Epilimnetic Supersaturation: A significant calibration challenge was the model's under-prediction of oxygen supersaturation in the epilimnion (surface waters). Observed data shows DO concentrations periodically exceeding 120-130% saturation due to intense algal photosynthesis. While the model simulates oxygen production, it tends to dampen these extreme peaks. This discrepancy is a known and acceptable limitation in complex ecosystem modeling and stems from several factors:

Fixed Photosynthetic Ratios: The model uses a standard photosynthetic quotient (oxygen produced per carbon fixed), which may be lower than the actual efficiency of algal communities during peak bloom conditions (Matsumoto 2021) (S. A. Wells 2017).

Gas Exchange Dynamics: The model's empirical formulas for air-water gas exchange may not fully capture the rapid oxygen accumulation that occurs on calm, sunny days when photosynthesis outpaces evasion to the atmosphere.

Spatial Heterogeneity: The two-dimensional model averages conditions laterally and cannot resolve localized "hotspots" of extremely dense algal patches where the highest supersaturation likely occurs.

Calibration Conclusion: Since the primary objective for the DO calibration was to accurately simulate hypolimnetic anoxia to drive internal nutrient loading—a process the model captures very well—the under-prediction of surface supersaturation was deemed an acceptable limitation for the purposes of this study.

3.2.7.1 Four Mile Hole 209

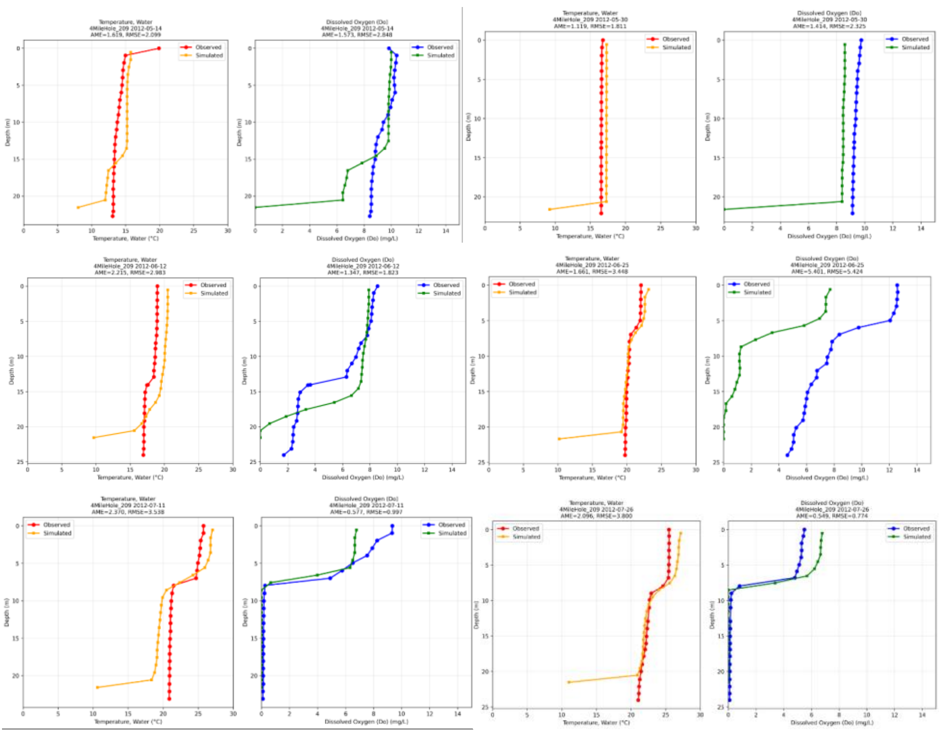

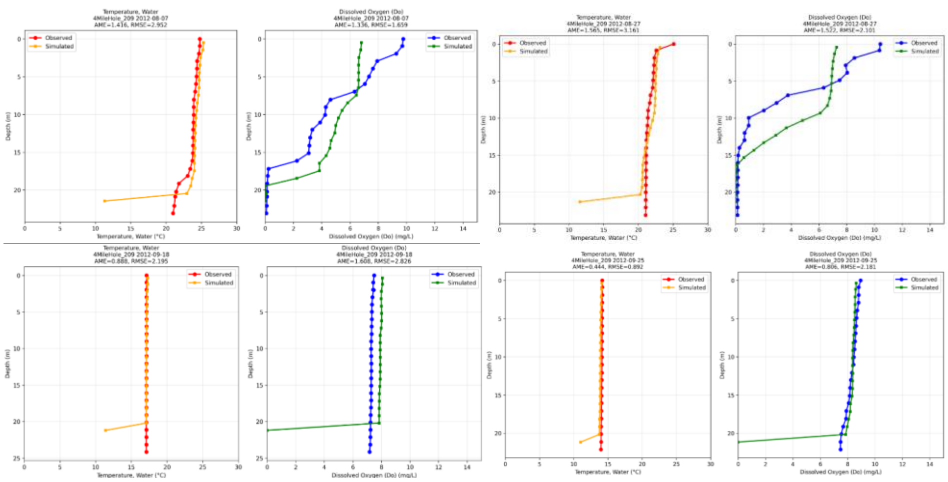

Figure 29. Temperature and DO Profiles - Observed vs. Simulated for 2012 at Four Mile Hole 209

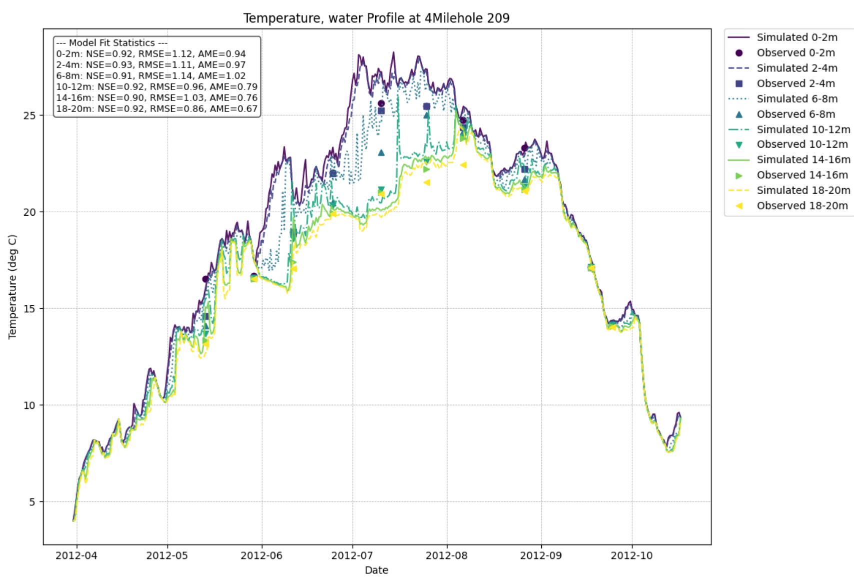

Figure 30. Model Calibration (2012) Time-Series for Water Temperature at Four Mile Hole 209

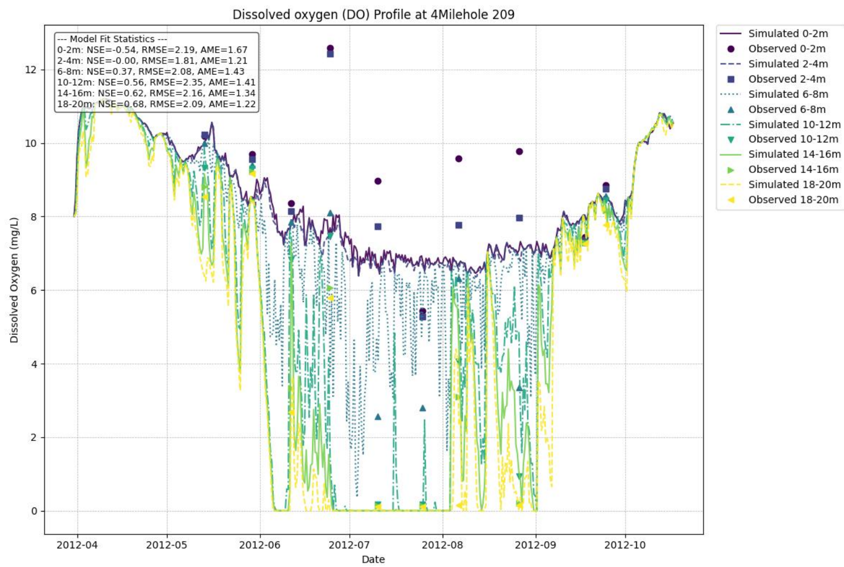

Figure 31. Model Calibration (2012) Time-Series for Dissolved Oxygen at Four Mile Hole 209

3.2.7.2 Lindberg

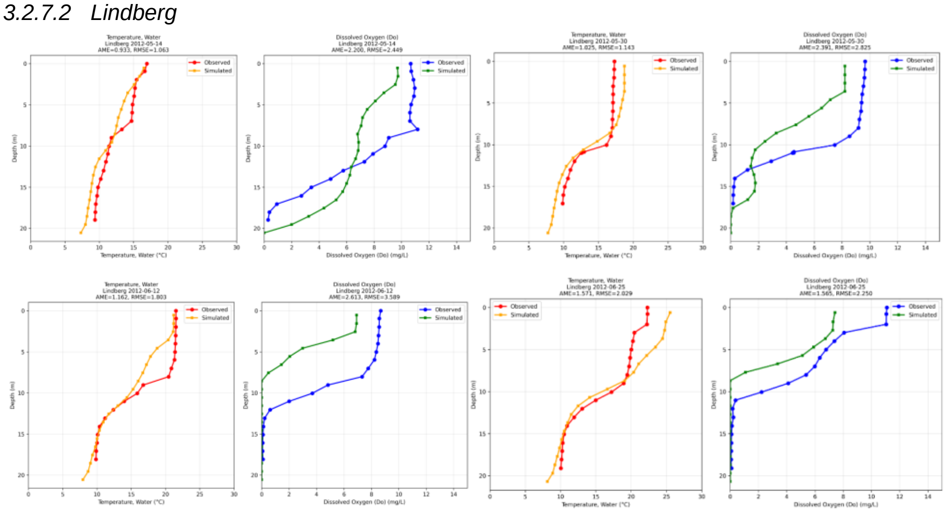

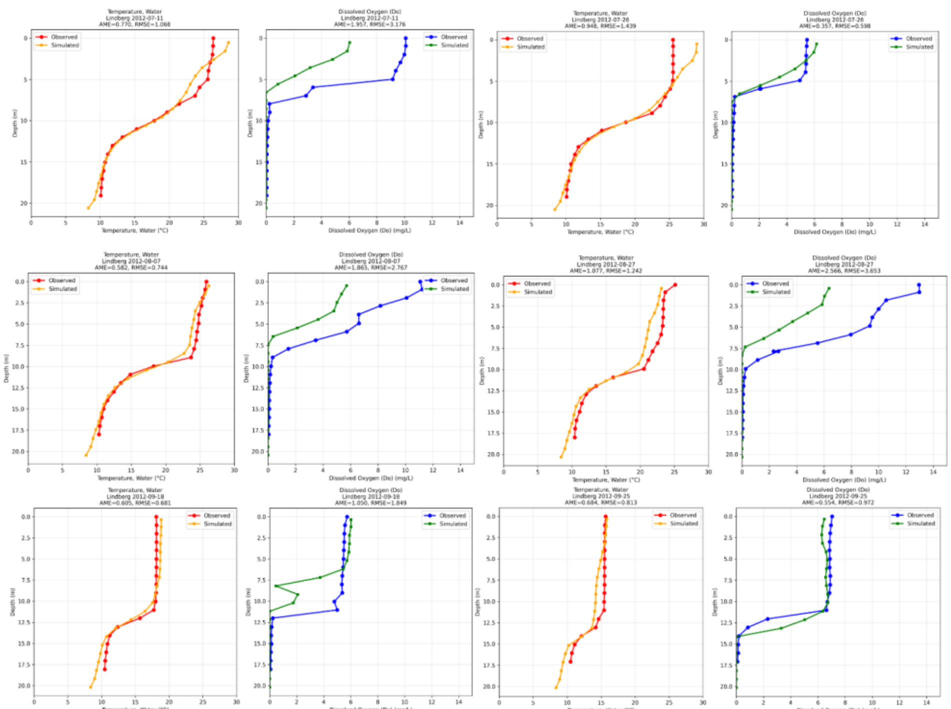

Figure 32. Temperature and DO Profiles - Observed vs. Simulated for 2012 at Lindberg

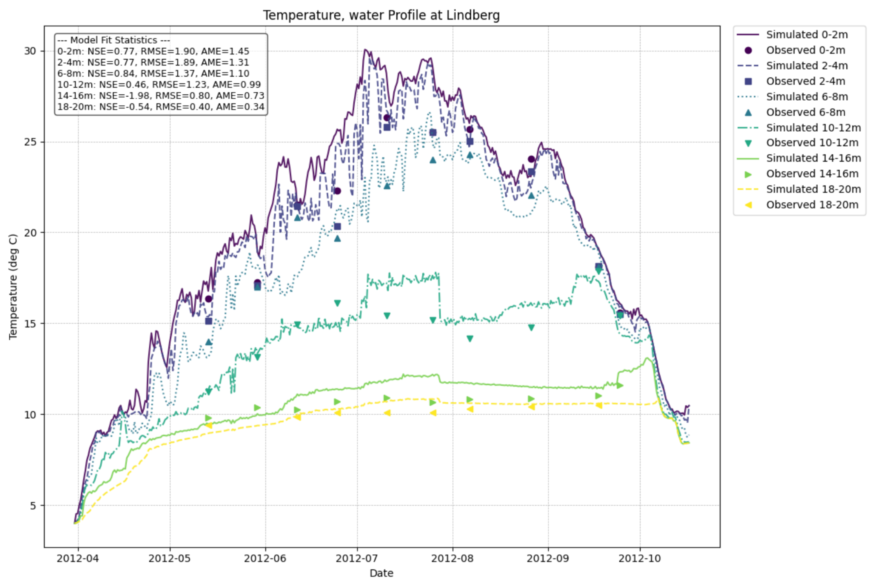

Figure 33. Model Calibration (2012) Time-Series for Water Temperature at Lindberg

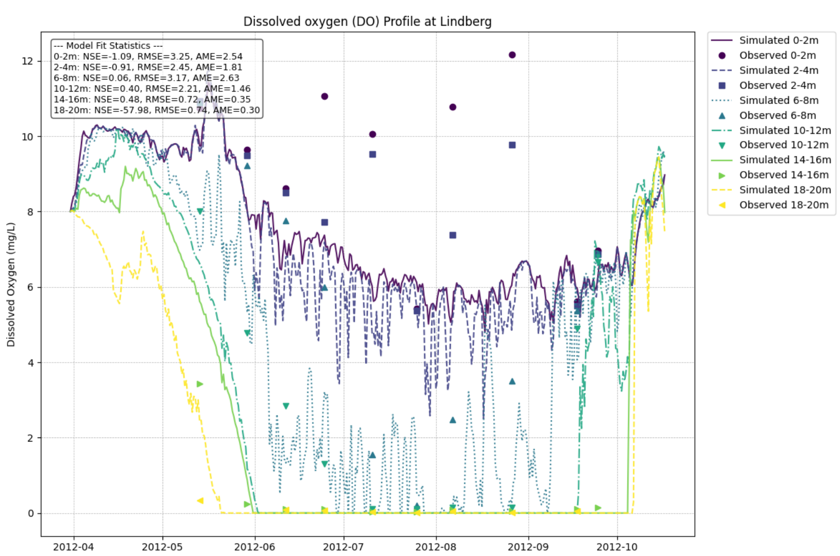

Figure 34. Model Calibration (2012) Time-Series for Dissolved Oxygen at Lindberg

3.2.8 Chlorophyll-a

Chlorophyll-a (Chl-a), the primary proxy for phytoplankton biomass, was a critical focus of the water quality calibration. As the key indicator of algal blooms and the lake's trophic state, accurately simulating Chl-a is essential for evaluating the effectiveness of management alternatives.

The primary calibration objective was to ensure the model accurately captured the seasonal *succession* of the algal community, rather than perfectly replicating the magnitude of every observed peak. As shown in Figure 35 and Figure 36, the model successfully reproduces the general timing of the spring diatom bloom and the subsequent shift to cyanobacteria dominance in late summer. This confirms that the model's underlying nutrient and light dynamics are simulating the key drivers of algal community structure.

A common and expected challenge in complex ecosystem modeling is the under-prediction of absolute Chl-a peak concentrations. While the simulated results capture the trend of algal blooms, they are often lower than the highest observed sample values. This discrepancy arises because a two-dimensional, laterally-averaged model cannot resolve localized, surface-level algal "hotspots" that are often targeted during field sampling.

Therefore, while predicting the exact peak biomass of dynamic algal blooms is a known modeling limitation, the model's demonstrated ability to capture the seasonal timing and relative response of the algal community provides a reliable and scientifically sound basis for comparing management scenarios.

3.2.8.1 Four Mile Hole 209

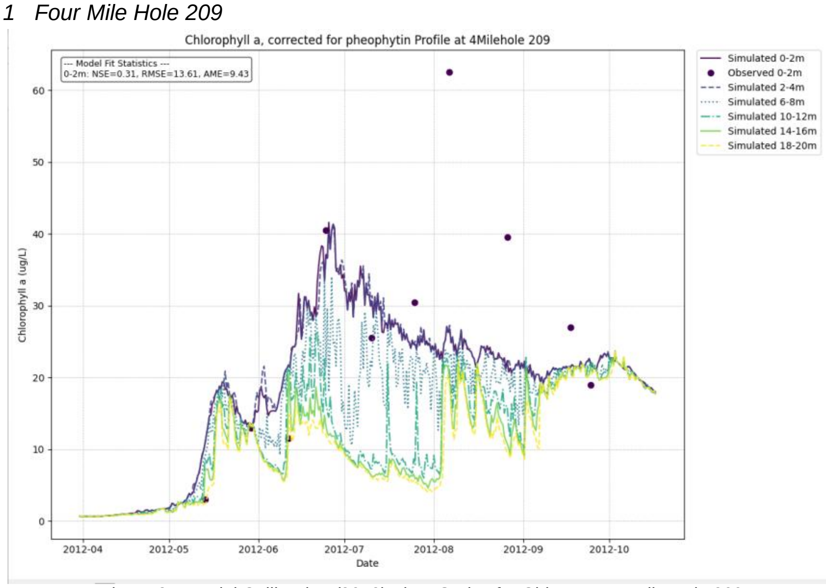

Figure 35. Model Calibration (2012) Time-Series for Chl a at Four Mile Hole 209

3.2.8.2 Lindberg

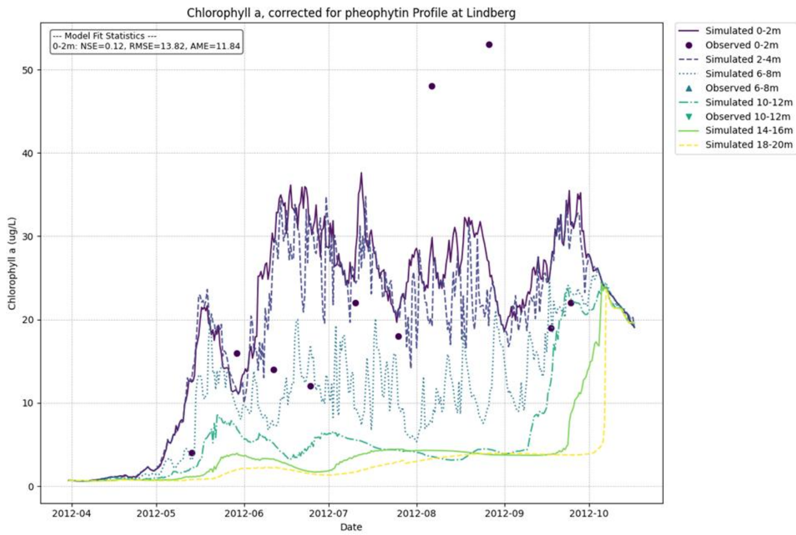

Figure 36. Model Calibration (2012) Time-Series for Chl a at Lindberg

3.2.9 Phosphorus

Phosphorus is the primary limiting nutrient controlling algal productivity in Lake Osakis. Therefore, the model's ability to accurately simulate the phosphorus cycle is fundamental to its utility as a management tool. The calibration focused on the model's capacity to replicate two opposing, yet interconnected, processes that define the lake's phosphorus dynamics:

1. Epilimnetic Depletion: The model was assessed on its ability to simulate the depletion of bioavailable orthophosphate (PO_4) in the surface waters during the growing season. This process is driven by the uptake of phosphorus by phytoplankton during algal blooms.
2. Hypolimnetic Accumulation: More critically, the calibration focused on reproducing the accumulation of orthophosphate in the anoxic bottom waters (hypolimnion) during summer stratification. This internal loading from lake sediments is a dominant driver of the lake's overall eutrophic condition.

As demonstrated in the time-series comparisons for the Four Mile Hole and Lindberg sites (Figure 37 and Figure 38), the model successfully captures both of these key dynamics. The simulated results accurately show the seasonal drawdown of surface PO_4 and, most importantly, replicate the timing and magnitude of phosphorus release from the sediments following the onset of anoxia. This successful calibration confirms that the model provides a robust representation of the internal phosphorus cycle, lending high confidence to its use in evaluating management alternatives.

3.2.9.1 Four Mile Hole 209

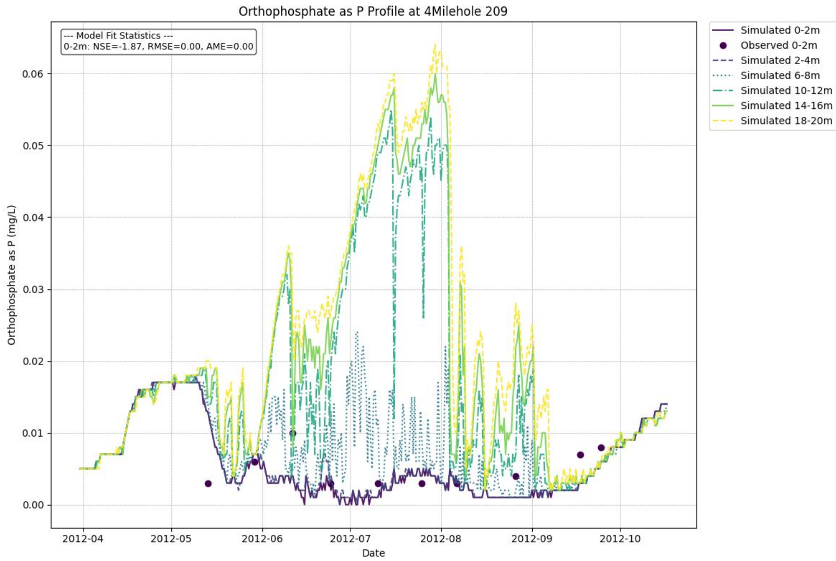

Figure 37. Model Calibration (2012) Time-Series for PO4 at Four Mile Hole 209

3.2.9.2 Lindberg

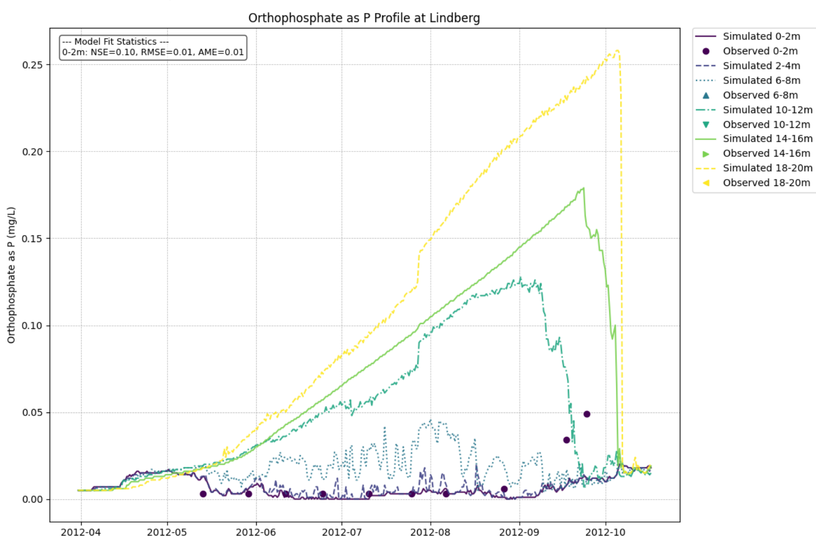

Figure 38. Model Calibration (2012) Time-Series for PO4 at Lindberg

3.2.10 Nitrogen

While phosphorus is the primary limiting nutrient in Lake Osakis, nitrogen plays a significant secondary role in the lake's biogeochemical cycle. Its different forms, primarily ammonium (NH4) and nitrate (NO3)—can influence the composition of the algal community and represent a significant component of the overall oxygen demand through the process of nitrification. Therefore, accurately simulating the nitrogen cycle is crucial for a balanced model.

To maintain consistency with the observed field data, which is reported by laboratories as "Ammonia-nitrogen as N," the model's simulated ammonium (NH4) concentrations are compared directly to these field measurements. Because ammonium constitutes the vast majority of total ammonia at the ambient pH ranges observed in Lake Osakis, these terms are treated as functionally equivalent for calibration comparisons and are reported as Ammonium-nitrogen as N (mg/L).

The nitrogen calibration focused on the model's ability to reproduce two key transformations observed in the lake:

- Nitrate Drawdown: The seasonal depletion of nitrate in the surface waters due to uptake by phytoplankton during the growing season.
- Ammonium Regeneration: The accumulation of ammonium in the anoxic bottom waters, driven by the decomposition of settled organic matter.

As shown in the time-series comparisons at both the Four Mile Hole and Lindberg sites (Figure 39 and Figure 40), the model effectively captures these seasonal dynamics. The simulated results track the observed pattern of nitrate depletion during the summer and the corresponding increase in ammonium concentrations in the hypolimnion.

This successful calibration of the nitrogen cycle is important for two reasons. First, it confirms that the model maintains a balanced nutrient budget for both phosphorus and nitrogen. Second, by accurately simulating nitrification (the conversion of ammonium to nitrate), it validates a key chemical oxygen sink, which enhances the credibility of the overall dissolved oxygen simulation.

3.2.10.1 Four Mile Hole 209

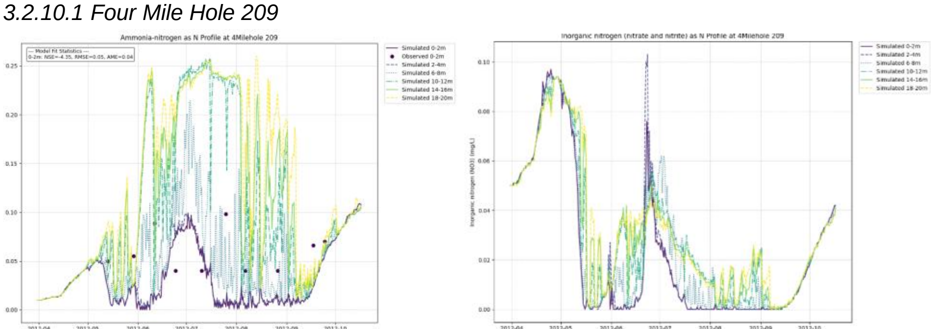

Figure 39. Model Calibration (2012) Time-Series for NH4 and NO3 at Four Mile Hole 209

3.2.10.2 Lindberg

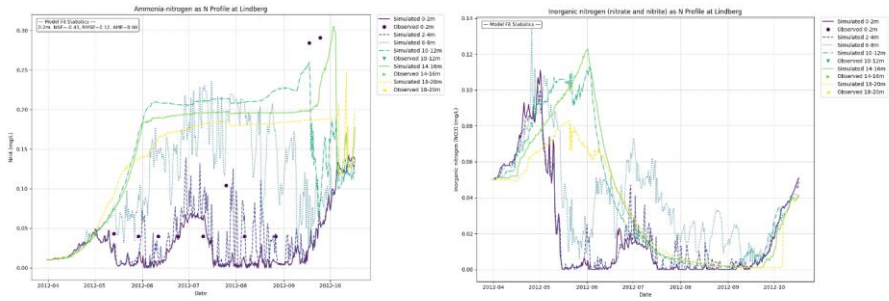

Figure 40. Model Calibration (2012) Time-Series for NH4 and NO3 at Lindberg

3.2.11 Total Suspended Solids

Total Suspended Solids (TSS) are a critical water quality parameter in Lake Osakis as they directly impact water clarity and light availability. In the model, TSS represents a composite of multiple simulated components, including:

- Inorganic Suspended Solids (ISS): Primarily clay and silt particles delivered from the watershed.
- Organic Solids: Particulate matter derived from both living phytoplankton and decaying particulate organic matter (POM) or detritus.

Evaluating the model's performance for TSS therefore serves as a comprehensive, integrated test of several core model functions: watershed loading, internal mixing dynamics, sediment transport, and biological production.

The time-series plots for the Four Mile Hole and Lindberg sites (Figure 41 and Figure 42) demonstrate that the model successfully reproduces the seasonal pattern of TSS concentrations. The simulated results capture the baseline levels and show a reasonable response to external loading events, aligning well with the observed data. This performance indicates that the model provides a credible representation of the complex particulate matter dynamics that ultimately govern water clarity in Lake Osakis.

3.2.11.1 Four Mile Hole 209

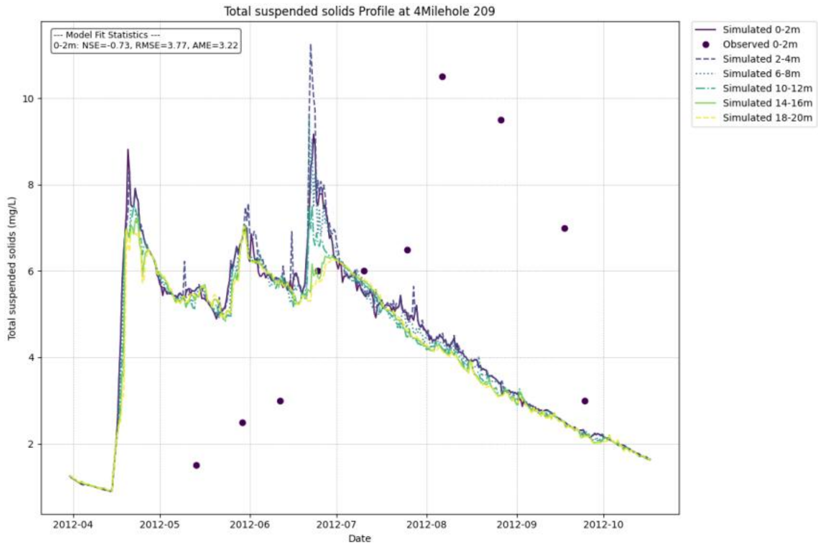

Figure 41. Model Calibration (2012) Time-Series for TSS at Four Mile Hole 209

3.2.11.2 Lindberg

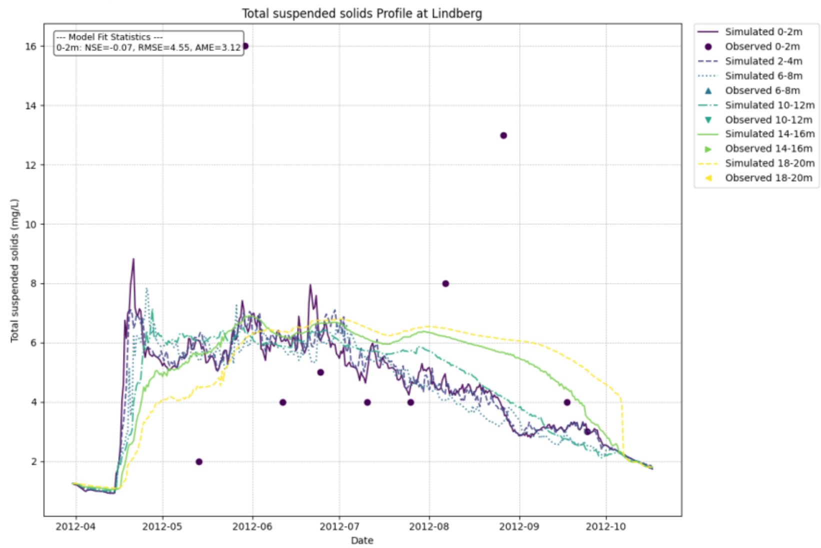

Figure 42. Model Calibration (2012) Time-Series for TSS at Lindberg

3.3 Model Validation

Following the successful calibration using 2012 data, the model's predictive capability was validated against a 20-year period from 1996 to 2015. This crucial step assesses the model's robustness by testing its ability to reproduce observed lake dynamics under a much wider range of hydrologic and meteorological conditions. For the verification run, the calibrated model coefficients were held constant; only the external drivers (e.g., meteorology and tributary inflows) were updated for each year.

The model's performance was evaluated by comparing simulated results against the full historical dataset from all three primary monitoring stations: Four Mile Hole (Sites 102 & 209) and Lindberg (Site 203), as shown in Figures 43-64.

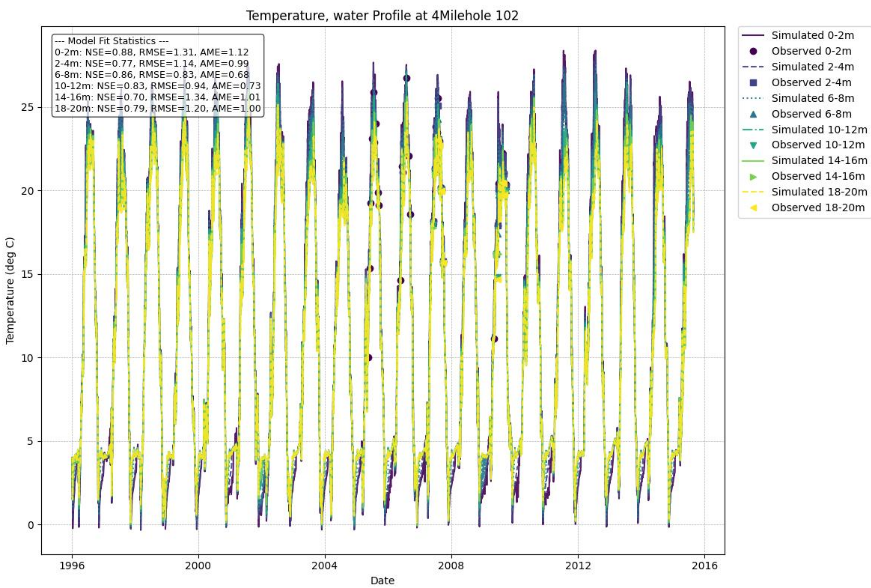

Figure 43. Model Verification (1996-2015) Time-Series for Temperature at Four Mile Hole 102

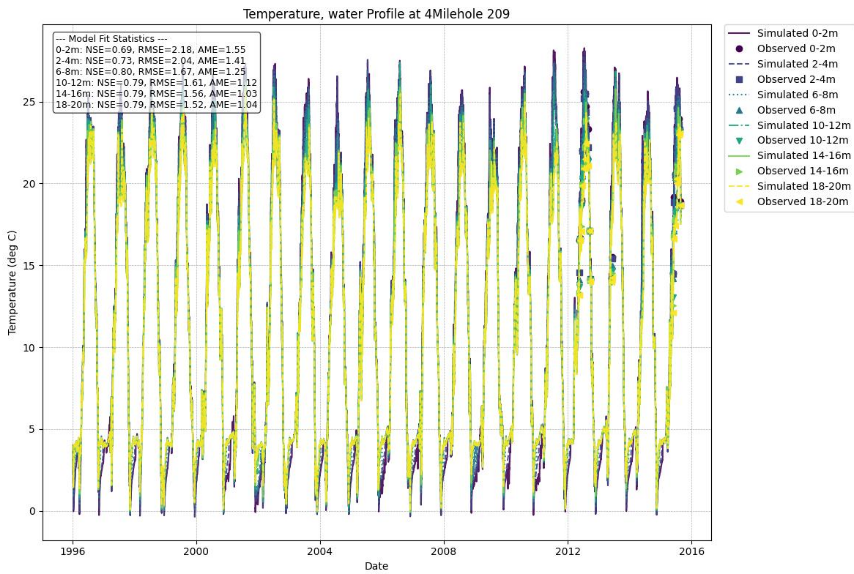

Figure 44. Model Verification (1996-2015) Time-Series for Temperature at Four Mile Hole 209

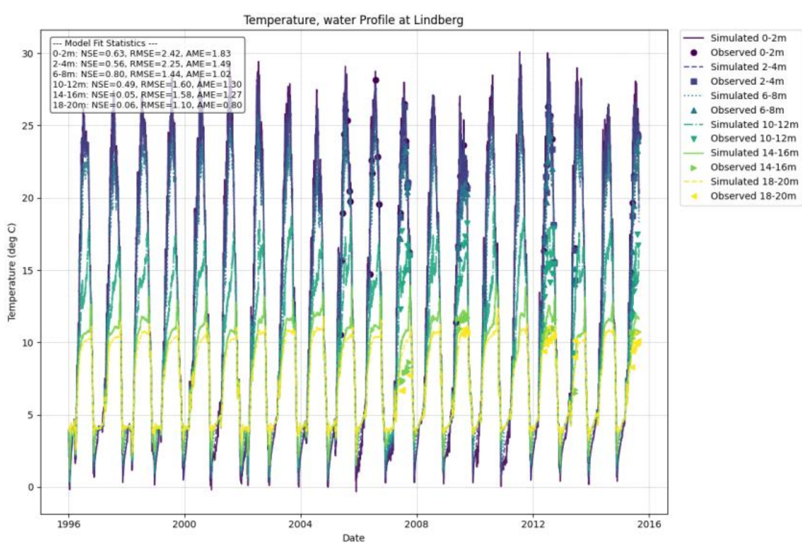

Figure 45. Model Verification (1996-2015) Time-Series for Temperature at Lindberg

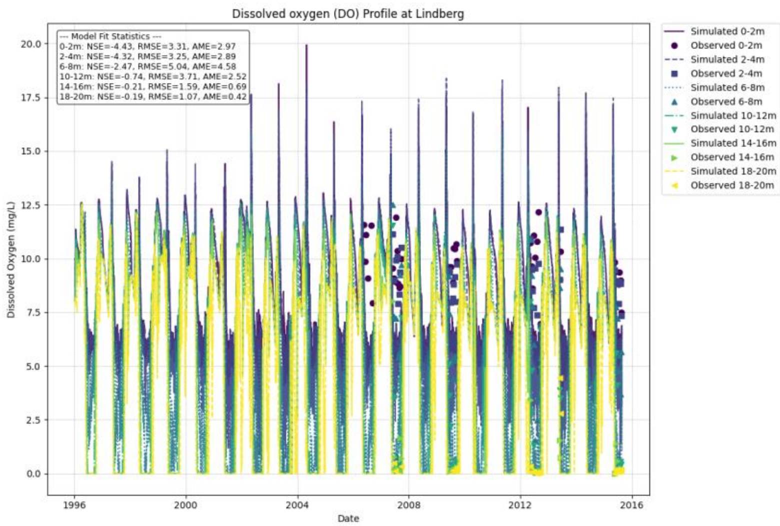

Figure 46 Model Verification (1996-2015) Time-Series for D.O. at Lindberg

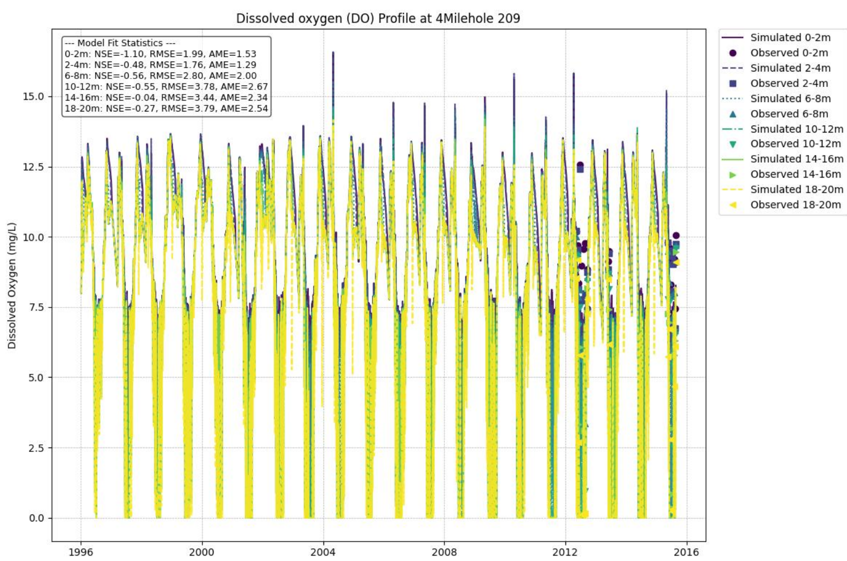

Figure 47. Model Verification (1996-2015) Time-Series for D.O. at Four Mile Hole 209

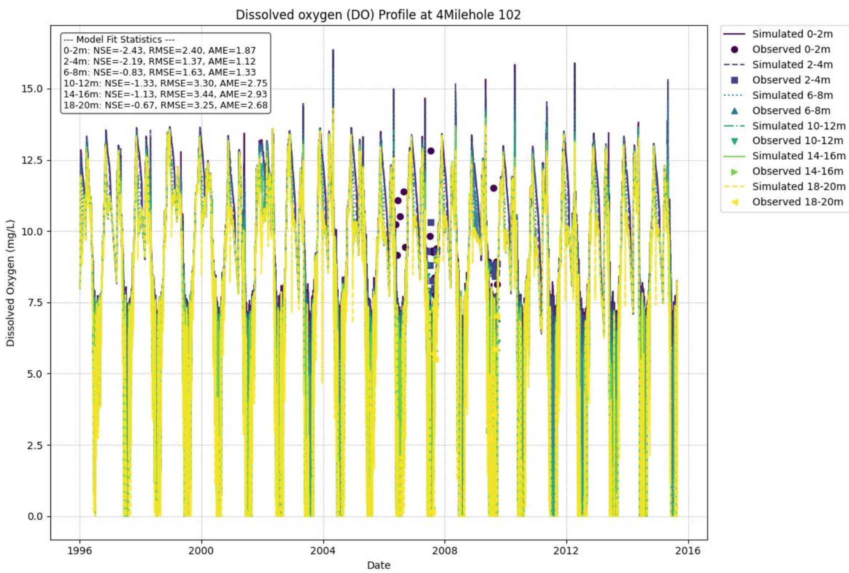

Figure 48. Model Verification (1996-2015) Time-Series for D.O. at Four Mile Hole 102

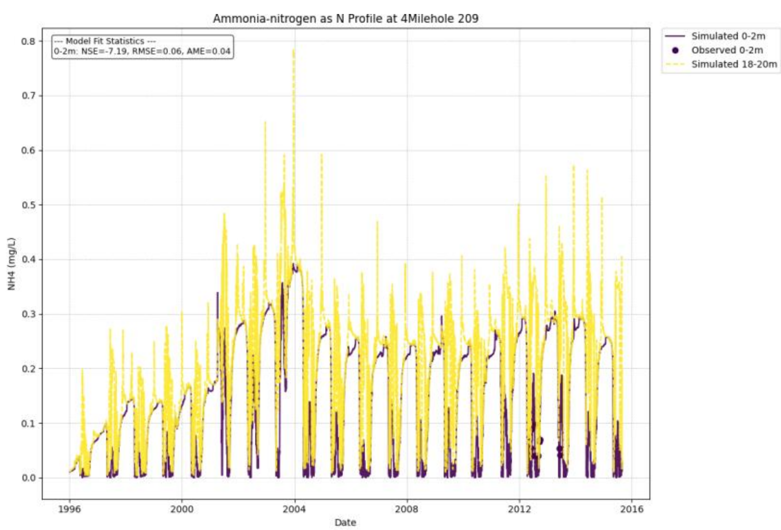

Figure 49. Model Verification (1996-2015) Time-Series for NH4 at Four Mile Hole 209

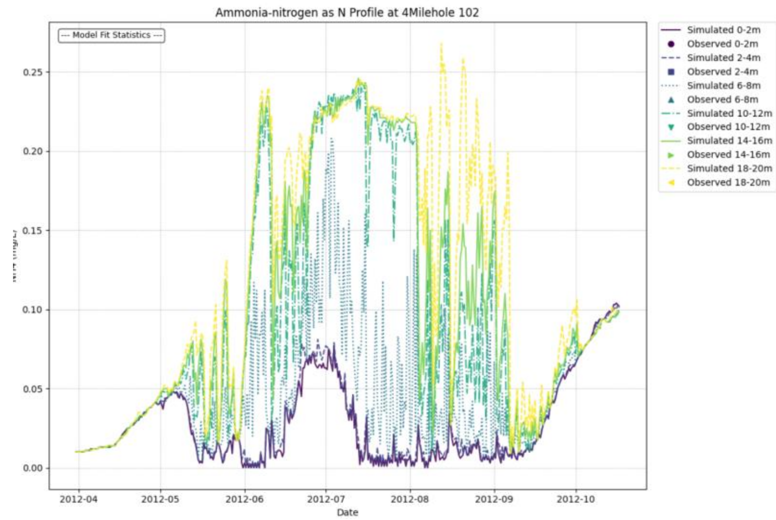

Figure 50. Model Verification (1996-2015) Time-Series for NH4 at Four Mile Hole 102

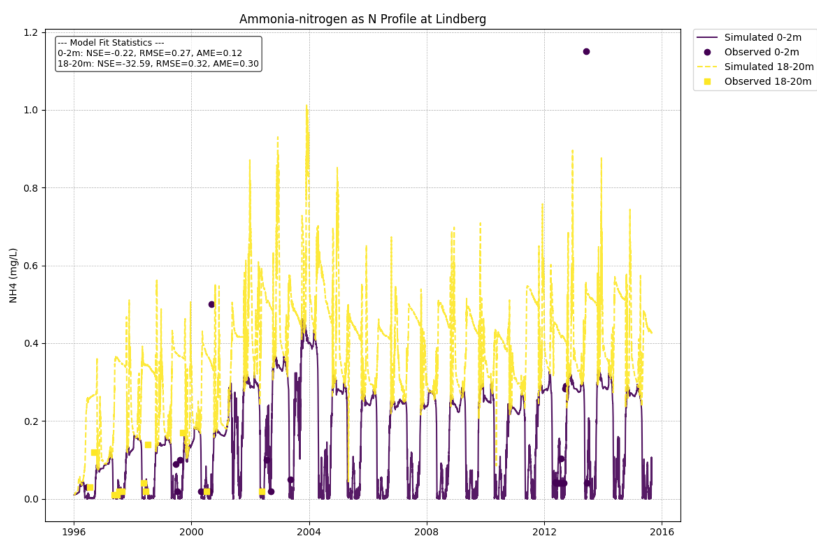

Figure 51. Model Verification (1996-2015) Time-Series for NH4 at Lindberg

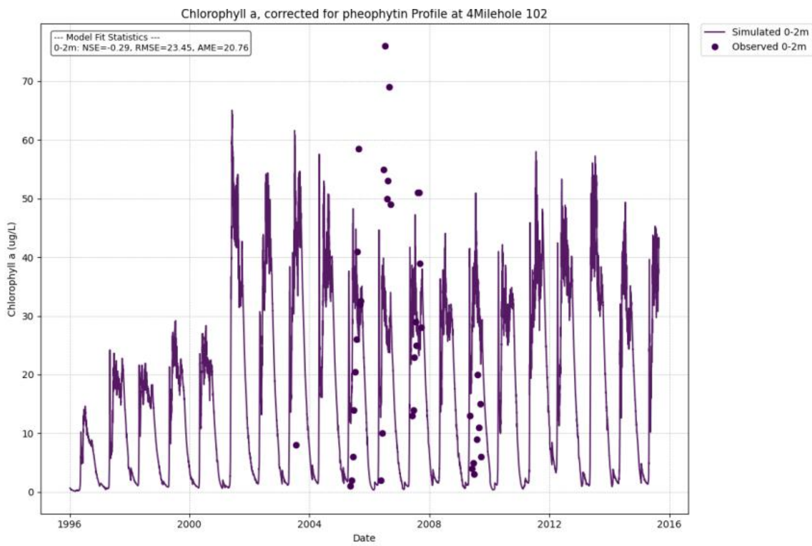

Figure 52. Model Verification (1996-2015) Time-Series for CHL a at Four Mile Hole 102

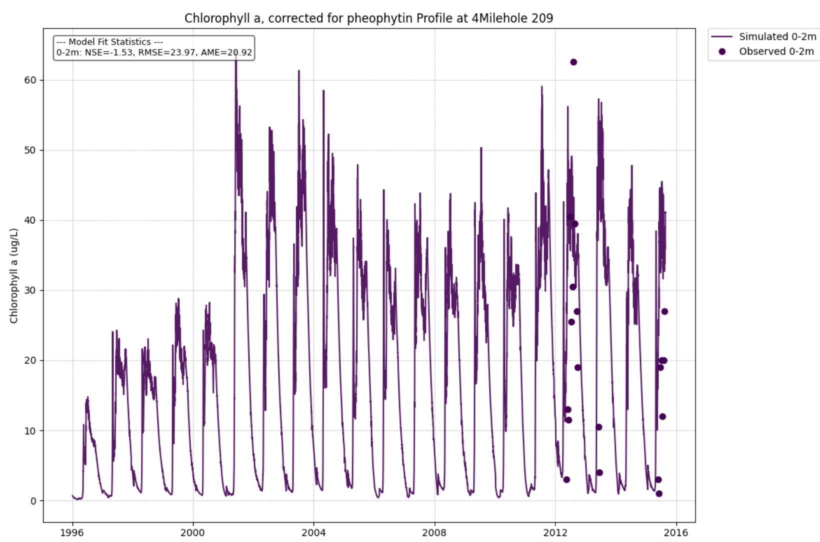

Figure 53. Model Verification (1996-2015) Time-Series for CHL a at Four Mile Hole 209

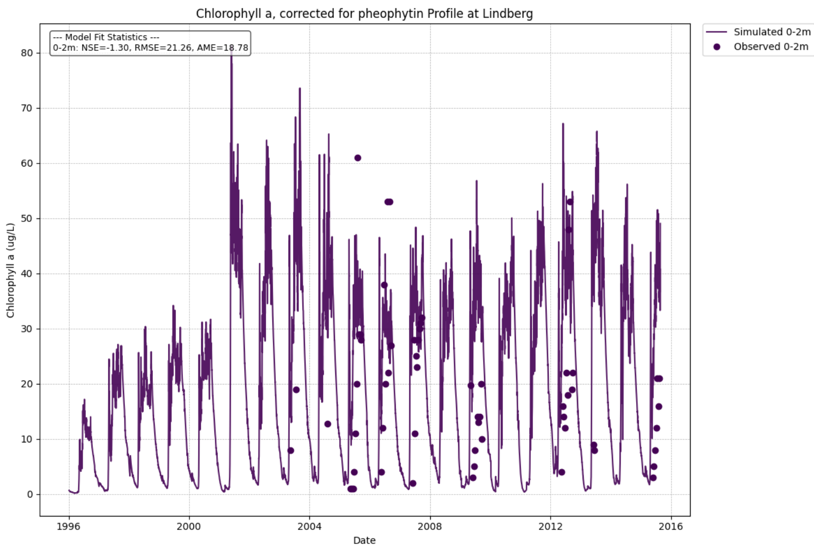

Figure 54. Model Verification (1996-2015) Time-Series for CHL a at Lindberg

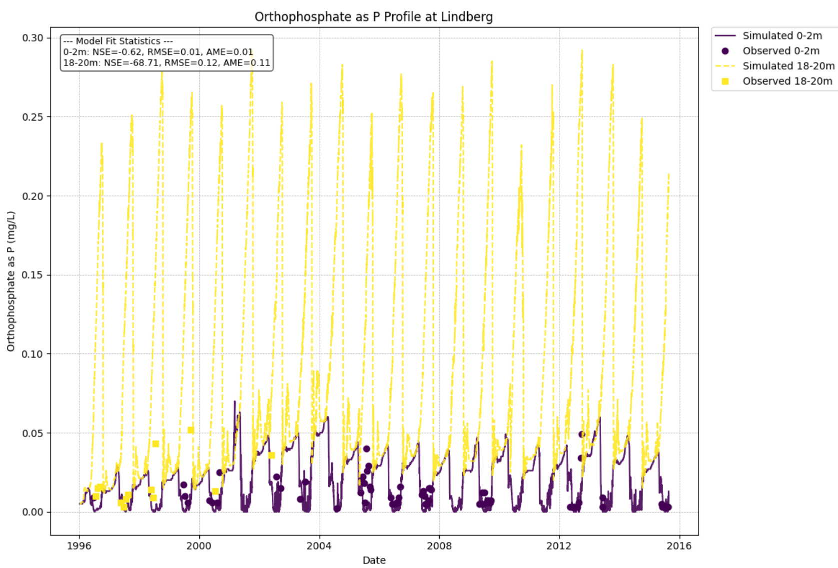

Figure 55. Model Verification (1996-2015) Time-Series for PO4 at Lindberg

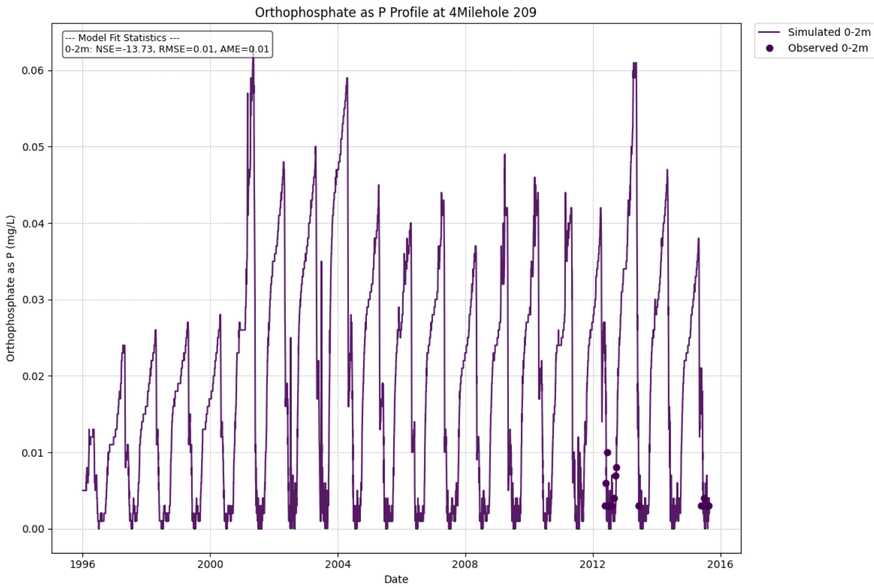

Figure 56. Model Verification (1996-2015) Time-Series for PO4 at Four Mile Hole 209

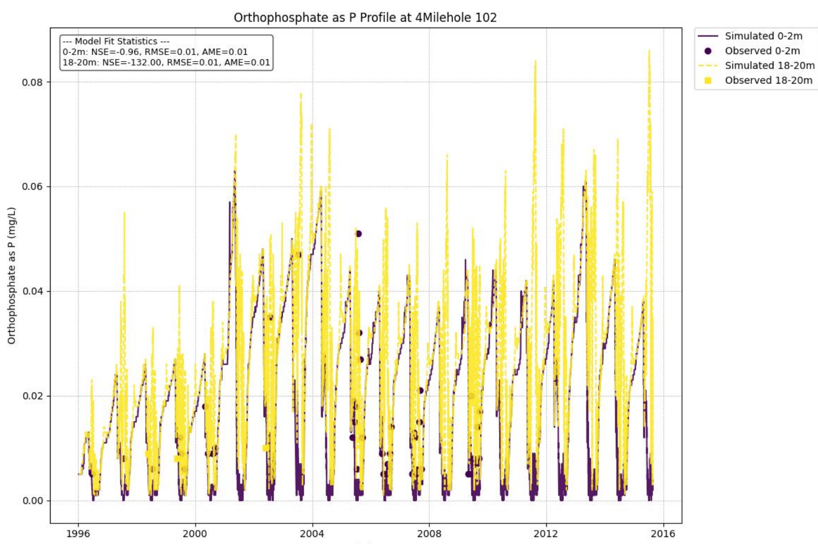

Figure 57. Model Verification (1996-2015) Time-Series for PO4 at Four Mile Hole 102

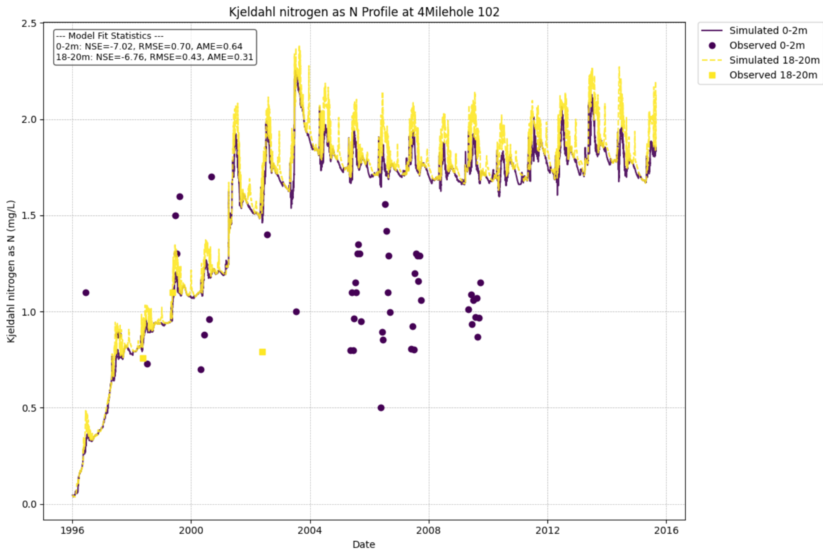

Figure 58. Model Verification (1996-2015) Time-Series for TKN at Four Mile Hole 102

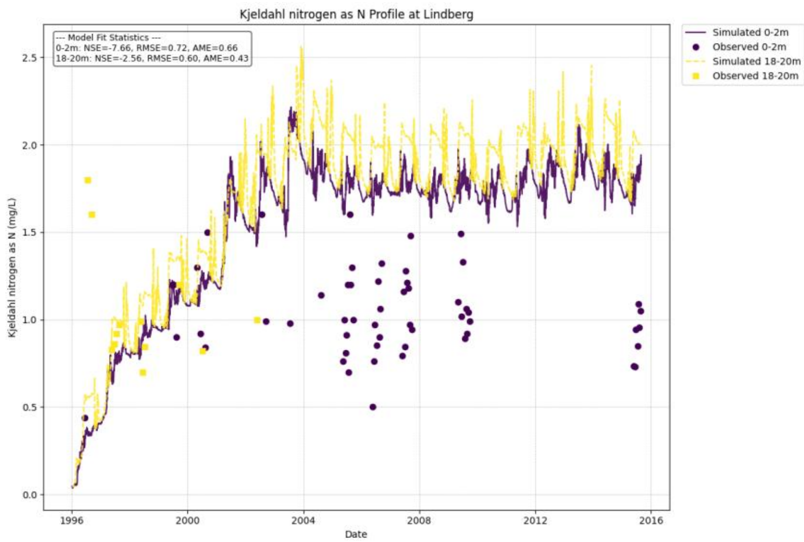

Figure 59. Model Verification (1996-2015) Time-Series for TKN at Lindberg

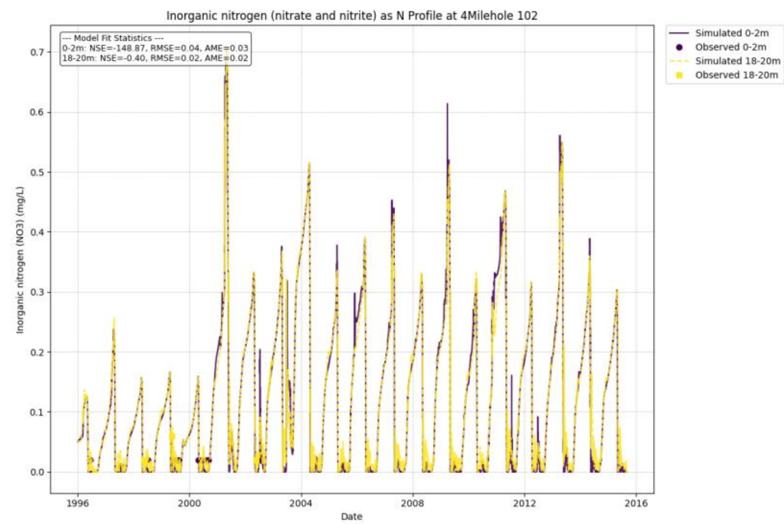

Figure 60. Model Verification (1996-2015) Time-Series for NO3NO2 at Four Mile Hole 102

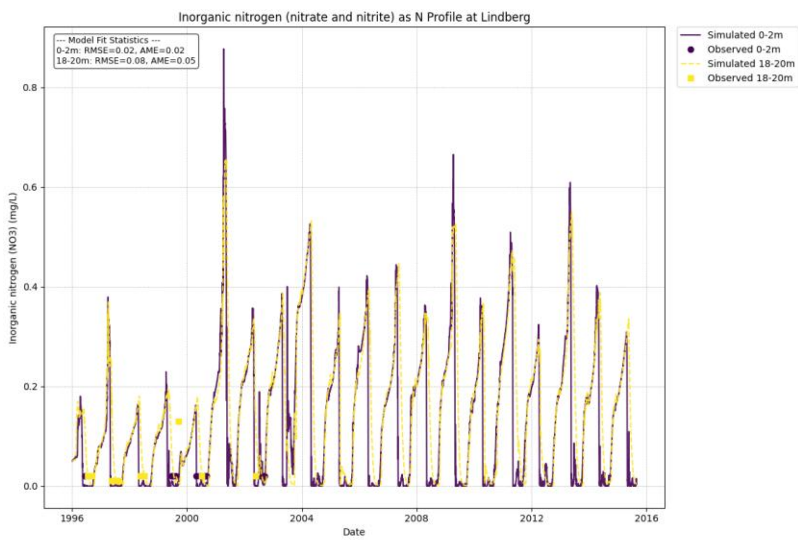

Figure 61. Model Verification (1996-2015) Time-Series for NO3NO2 at Lindberg

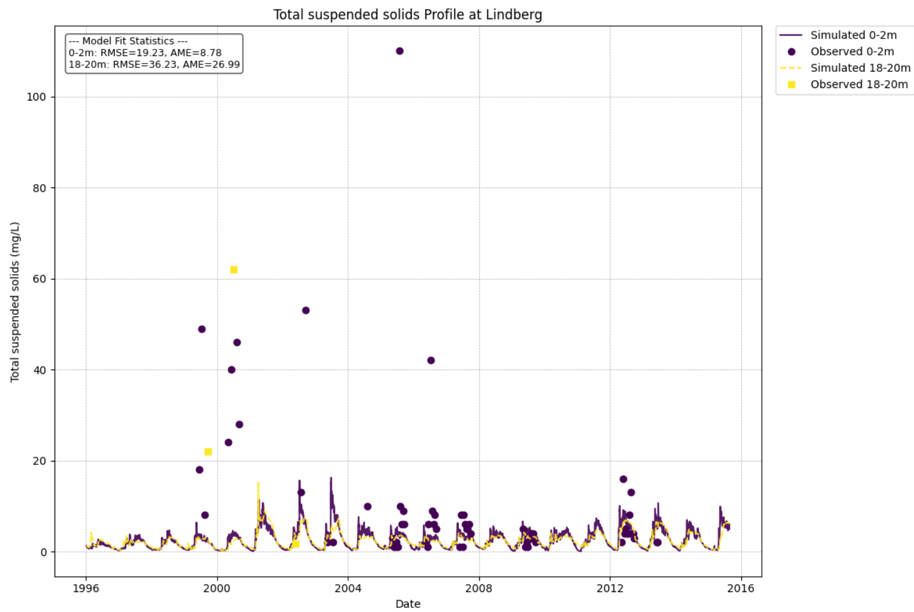

Figure 62. Model Verification (1996-2015) Time-Series for TSS at Lindberg

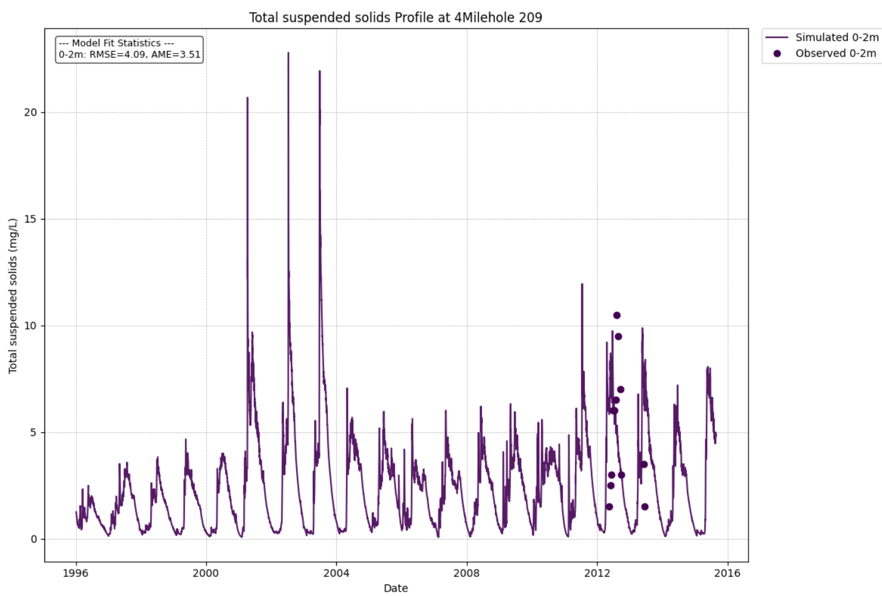

Figure 63. Model Verification (1996-2015) Time-Series for TSS at Four Mile Hole 209

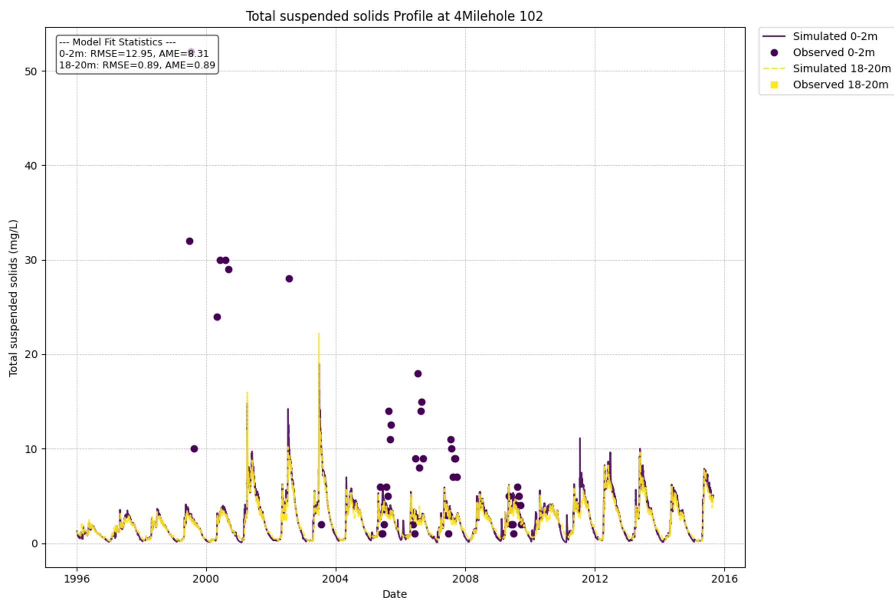

Figure 64. Model Verification (1996-2015) Time-Series for TSS at Four Mile Hole 102

3.3.1 Calibration and Verification Summary

The overall model performance is strong for key physical and chemical parameters, particularly Temperature and Orthophosphate (PO_4), which consistently meet the stringent calibration targets across both periods. Performance for biological and organically-driven parameters like Chlorophyll-a and Ammonia (NH_4) is weaker, which is a common and expected outcome in complex ecosystem models.

- Calibration (2012): The model demonstrates a strong fit to the 2012 data, meeting the Mean Absolute Error (MAE) targets for most primary variables. This confirms the underlying parameter set is sound. The detailed statistics for the calibration period are provided in Table 19 and Table 21.
- Verification (1996-2015): The verification shows a slight but expected degradation in performance compared to the calibration year. This is normal, as the model is now being tested against two decades of varied conditions. Importantly, the model remains robust for Temperature and key nutrients, validating its core hydrodynamic and biogeochemical framework. The detailed statistics for the full verification period are provided in Table 20 and Table 22.

Commented [SK4]: Probably good to reference tables 18 and 19 too.

Key Performance Takeaways:

- Model Strengths: The model is highly reliable for simulating Temperature, Orthophosphate, and Nitrate + Nitrite. This success provides high confidence in the model's ability to simulate physical structure (stratification) and the foundational nutrient pathways that drive the lake's ecology.

- Model Weaknesses: The model has significant difficulty simulating the absolute magnitude of biological parameters. Chlorophyll-a is the most problematic, with errors exceeding the target. This indicates that while the model captures the timing of algal blooms, it cannot precisely predict their peak density—a known challenge in laterally-averaged models. Performance for Ammonia and Total Kjeldahl Nitrogen is also weak, linked to the complexities of organic matter decay and algal metabolism.

Despite these limitations, the calibrated and validated model is scientifically sound and fit-for-purpose. Its strong performance on the key physical and chemical drivers makes it a reliable tool for evaluating the *relative* change between different management alternatives.

Table 19. Model's performance during the calibration summary

Variable	**Target AME**	**Performance Summary**	**Status**
Temperature	< 1.0 °C	Met the target at 5 of 8 locations/depths. Slightly exceeded at Lindberg surface and 4-mile hole mid-depths.	Largely Met
Dissolved Oxygen	< 2.0 mg/L	Met the target at 7 of 8 locations/depths. Exceeded only at the Lindberg surface (2.58 mg/L).	Largely Met
Ammonia (NH4)	< 0.03 mg/L	Failed to meet the target at both measured locations (0.04 and 0.08 mg/L).	Not Met
Chlorophyll a	< 10.0 µg/L	failed to meet the target at one location (11.32 and 9.60 µg/L).	Not Met
Orthophosphate (PO4)	< 0.01 mg/L	Met the target at both measured locations (0.00 and 0.01 mg/L).	Met

Table 20. Model's performance during the verification (1996-2015)

Variable	Target AME	Performance Summary	Status
Temperature	< 1.0 °C	Met the target at 5 of 18 locations/depths. Performance is best at mid-to-bottom depths. Surface layers consistently exceed the target.	Partially Met
Dissolved Oxygen	< 2.0 mg/L	Met the target at 9 of 18 locations/depths. Performance is poor in deeper waters at 4-mile hole sites and surface/mid-depths at Lindberg.	Partially Met
Ammonium (NH4)	< 0.03 mg/L	Failed to meet the target at all 5 measured locations.	Partially Met
Chlorophyll a	< 10.0 µg/L	Significantly failed to meet the target at all 3 locations, with AME values >2x the target.	Met
Orthophosphate (PO4)	< 0.01 mg/L	Met the target at 4 of 5 locations/depths. Only exceeded at Lindberg deep water (0.11 mg/L).	Largely Met
Total Kjeldahl Nitrogen	< 0.4 mg/L	Failed to meet the target at all 5 measured locations.	Not Met
Nitrate + Nitrite (NOx)	< 0.1 mg/L	Met the target at all 4 measured locations/depths.	Met

Table 21. Model's performance statistics during the calibration (2012)

Calibration (2012) Parameter	Site	Depth	AME	RMSE	N_Comparisons
Temperature, water (Deg C)	4milehole_209	0-2m	0.94	1.11	10
		2-4m	1.00	1.13	10
		6-8m	1.06	1.19	10
		10-12m	0.83	0.99	10
		14-16m	0.80	1.05	10
		18-20m	0.67	0.88	10
	Lindberg	0-2m	1.44	1.88	10
		2-4m	1.32	1.90	10
		6-8m	1.11	1.37	10
		10-12m	0.96	1.21	10
		14-16m	0.69	0.76	10
		18-20m	0.32	0.39	8
Dissolved oxygen (DO) (mg/l)	4milehole_209	0-2m	1.69	2.28	10
		2-4m	1.21	1.84	10
		6-8m	1.44	2.07	10
		10-12m	1.48	2.37	10
		14-16m	1.44	2.15	10
		18-20m	1.27	2.07	10
	Lindberg	0-2m	2.58	3.30	10
		2-4m	1.77	2.35	10
		6-8m	2.32	2.81	10
		10-12m	1.42	2.12	10
		14-16m	0.38	0.76	10
		18-20m	0.31	0.75	8
Ammonium as N (mg/l)	4milehole_209	0-2m	0.04	0.05	10
	Lindberg	0-2m	0.08	0.12	10
Chlorophyll a, corrected for pheophytin (ug/l)	4milehole_209	0-2m	11.32	15.80	10
	Lindberg	0-2m	9.60	13.01	10
Orthophosphate as P (mg/l)	4milehole_209	0-2m	0.00	0.01	10
	Lindberg	0-2m	0.01	0.02	10
Total suspended solids (mg/l)	4milehole_209	0-2m	3.24	3.84	10
	Lindberg	0-2m	3.11	4.67	10

Table 22. Model's performance statistics during the verification (1996-2015)

Verification (1996-2015) Parameter	Site	Depth	AME	RMSE	N_Comparisons
Temperature, water (Deg C)	4milehole_102	0-2m	1.12	1.31	34
		2-4m	0.99	1.14	17
		6-8m	0.68	0.83	17
		10-12m	0.73	0.94	17
		14-16m	1.01	1.34	16
		18-20m	1.00	1.20	9
	4milehole_209	0-2m	1.55	2.18	21
		2-4m	1.41	2.04	21
		6-8m	1.25	1.67	21
		10-12m	1.12	1.61	21
		14-16m	1.03	1.56	21
		18-20m	1.05	1.52	20
	Lindberg	0-2m	1.83	2.42	53
		2-4m	1.49	2.25	36
		6-8m	1.02	1.44	36
		10-12m	1.30	1.60	35
		14-16m	1.27	1.58	34
		18-20m	0.80	1.10	25
Dissolved oxygen (DO) (mg/l)	4milehole_102	0-2m	1.87	2.40	23
		2-4m	1.12	1.37	17
		6-8m	1.34	1.63	17
		10-12m	2.75	3.30	17
		14-16m	2.93	3.44	16
		18-20m	2.68	3.25	9
	4milehole_209	0-2m	1.53	1.99	21
		2-4m	1.29	1.76	21
		6-8m	2.00	2.80	21
		10-12m	2.67	3.78	21
		14-16m	2.34	3.44	21
		18-20m	2.54	3.79	20
	Lindberg	0-2m	2.97	3.31	42

		2-4m	2.89	3.25	36
		6-8m	4.58	5.04	36
		10-12m	2.52	3.71	35
		14-16m	0.69	1.59	34
		18-20m	0.42	1.07	25
Ammonium as N (mg/l)	4milehole_102	0-2m	0.07	0.15	11
		14-16m	0.18	0.22	7
	4milehole_209	0-2m	0.04	0.06	12
	Lindberg	0-2m	0.12	0.27	23
		18-20m	0.30	0.32	12
Chlorophyll a, corrected for pheophytin (ug/l)	4milehole_102	0-2m	20.76	23.45	37
	4milehole_209	0-2m	20.92	23.97	19
	Lindberg	0-2m	18.78	21.26	58
Orthophosphate as P (mg/l)	4milehole_102	0-2m	0.01	0.01	48
		14-16m	0.01	0.02	8
	4milehole_209	0-2m	0.01	0.01	19
	Lindberg	0-2m	0.01	0.01	68
		18-20m	0.11	0.12	13
Kjeldahl nitrogen as N (mg/l)	4milehole_102	0-2m	0.64	0.70	48
		14-16m	0.95	0.99	7
	4milehole_209	0-2m	0.91	0.91	7
	Lindberg	0-2m	0.66	0.73	55
	Lindberg	18-20m	0.43	0.60	12
Inorganic nitrogen (nitrate and nitrite) as N (mg/l)	4milehole_102	0-2m	0.03	0.04	11
		14-16m	0.06	0.10	6
	Lindberg	0-2m	0.02	0.02	10
		18-20m	0.05	0.08	12
Total suspended solids (mg/l)	4milehole_102	0-2m	8.32	12.95	45
		14-16m	24.90	29.48	6
	4milehole_209	0-2m	3.51	4.09	12
	Lindberg	0-2m	8.78	19.23	60

4 Model Sensitivity Analysis

The sensitivity analysis for Lake Osakis was conducted to evaluate how uncertainty in key physical and biogeochemical parameters influences the model's simulated temperature, dissolved oxygen (DO), and nutrient dynamics. This analysis serves as the bridge between calibration and scenario testing—quantifying which processes most strongly shape lake behavior and where parameter refinement yields the greatest improvement in model performance.

In eutrophic systems like Lake Osakis, interactions between physical mixing, sediment fluxes, and algal growth dominate the seasonal cycle of oxygen and nutrient concentrations. Identifying which parameters most affect these linkages improves both confidence in calibration and interpretability of scenario results.

4.1 Methods

Sensitivity testing was performed using the automated Python workflow developed for this project. Each selected parameter was perturbed by ±20 percent relative to the calibrated (baseline) value while holding all other parameters constant. Simulations were conducted for key parameters governing:

- **Physical forcing:** wind-sheltering coefficient (WSC)
- **Light and optical conditions:** extinction coefficients for water and solids (EXA, EXSS, EXOM)
- **Sediment processes:** sediment oxygen demand (SOD) and sediment phosphorus release rate (PO4R)
- **Nutrient & organic loadings:** nitrogen, phosphorus and organic matter loading from the watershed.

4.2 Overview of Sensitivity Responses

The model sensitivity analysis indicates that the water quality dynamics of Lake Osakis are predominantly controlled by internal physical and biogeochemical processes, rather than by external nutrient inputs from the watershed. The key drivers identified are physical mixing (governed by the Wind Sheltering Coefficient, WSC) and internal nutrient loading from sediment (Sediment Oxygen Demand, SOD, and Sediment Phosphorus Release Rate, PO4R). The model's relative insensitivity to short-term changes in external loads is a direct consequence of the lake's long hydraulic residence time (approximately 5 years), which buffers its effects. This highlights the critical role of internal feedback loops between stratification, oxygen depletion, and sediment nutrient release in shaping the lake's seasonal behavior.

4.2.1 Sensitivity Heatmap Summary

The heatmap (Figure 65) highlights that:

- **WSC** influences nearly all state variables through mixing and surface exchange.
- **SOD** primarily affects hypolimnetic DO and indirectly influences PO_4 and CHLA through redox-mediated nutrient release.

- **PO4R** directly alters phosphorus and chlorophyll concentrations but has minimal effect on temperature or DO outside the stratified season.
- **Optical parameters (EXA, EXH$_2$O, EXSS)** moderate light limitation and algal productivity.

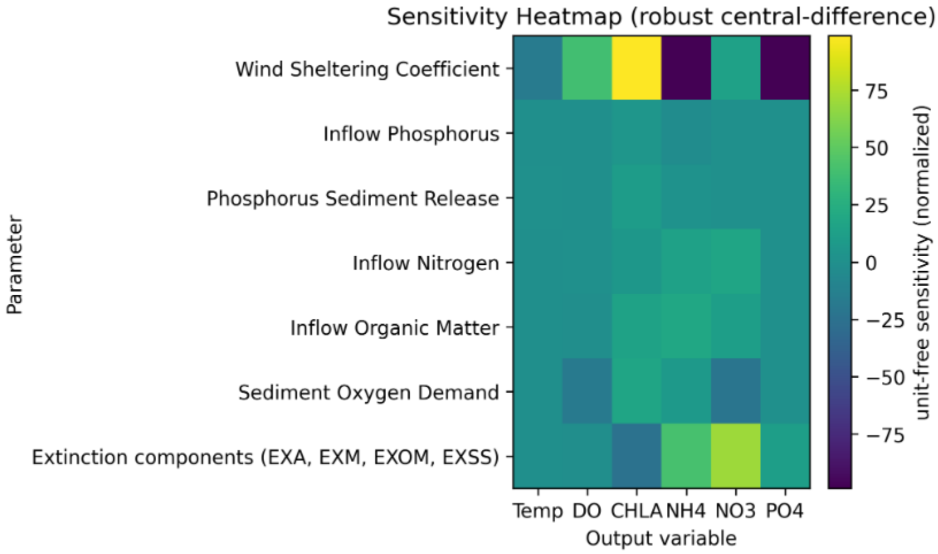

Figure 65. Parameter sensitivity heatmap (Δ% vs. baseline, ±20% perturbation). Chlorophyll a, orthophosphate (PO_4-P), ammonia (NH_4-N), and nitrate (NO_3-N) for each tested parameter.

4.2.2 Quantitative Sensitivity Tables

To quantify the visual trends established in the heatmap, Table 23 and Table 24 present the precise percent changes for key constituents across different model depths. These results mathematically confirm the dominance of internal processes. For instance, perturbing external watershed inputs (Inflow Phosphorus, Nitrogen, and Organic Matter) yielded nearly negligible responses, typically altering in-lake concentrations by less than 1% across most depths. In stark contrast, altering internal physical drivers like the Wind Sheltering Coefficient (WSC) drove double-digit percent changes in dissolved oxygen (up to 51.4% at depth) and chlorophyll-a. Similarly, altering Sediment Oxygen Demand (SOD) produced significant localized shifts in deep-water oxygen.

Table 23. Percent change of D.O. at different depths (Lindberg and Four Mile Hole 209 sites) to inputs changes of select parameters.

Parameter - Sensitivity Percent Change	Input_Change	DO 1m	DO 3m	DO 7m	DO 11m	DO 15m	DO 19m
Wind Sheltering Coefficient	-20	-5.3	-6.3	-9.8	-34	-38	-51.4
	20	4.6	4.8	5.5	11.4	12.6	15.6
Inflow Phosphorus	-20	0	0.2	0.1	0.1	0.6	0.5
	20	-0.1	0.2	0.1	-0.2	0.3	0.1
Phosphorus Sediment Release	-20	-0.2	0.1	0.1	0	0.5	0.4
	20	-0.2	-0.1	-0.1	-0.2	-0.5	-0.6
Inflow Nitrogen	-20	-0.1	0.2	0.2	-0.1	0.6	0.4
	20	0	0.2	0.1	0	0.3	0.5
Inflow Organic Matter	-20	0.1	0.5	0.2	0.2	1.1	0.6
	20	-0.1	0	0	-0.1	-0.2	-0.2
Sediment Oxygen Demand	-20	1.5	1.7	2.2	3.2	5.2	6.4
	20	-1.6	-1.7	-2	-3.7	-5.8	-7.8
Extinction components (EXA, EXM, EXOM, EXSS)	-20	0	0.3	0.1	0.5	0.3	0.1
	20	-0.1	0	0	-0.3	-0.1	-0.3

Table 24. Percent change of CHL a, PO4, NH4 and NO3 (Lindberg and Four Mile Hole 209 sites) to inputs changes of select parameters.

Parameter	Input_Change	CHLA	PO4	NH4	NO3
Wind Sheltering Coefficient	-20	-17.6	30	46.4	-16.5
	20	24	-15	-24.6	-10.9
Inflow Phosphorus	-20	-4	0	-1.1	0
	20	-1.3	0	-2.4	0
Phosphorus Sediment Release	-20	-2.4	0	0	0
	20	1.9	0	0.7	0
Inflow Nitrogen	-20	-4.1	0	-5.7	-7.2
	20	-1.4	0	0	0
Inflow Organic Matter	-20	-5.8	0	-7.7	-6.3
	20	0.7	0	0	0
Sediment Oxygen Demand	-20	-3.4	0	-0.7	2.9
	20	3.5	0	1.3	-5.9
Extinction components (EXA, EXM, EXOM, EXSS)	-20	3.8	-5	-7.7	-18.8
	20	-4.8	0	9.1	10.9

Increased wind exposure (a higher WSC value) enhances vertical mixing, which distributes nutrients more evenly but reduces light exposure near the surface, resulting in smaller, more stable algal blooms. Conversely, a lower WSC limits mixing and isolates surface water, allowing transient nutrient accumulation and intense surface blooms that rapidly collapse after nutrient depletion.

4.3 Interpretation and Calibration Implications

- **Wind forcing (WSC)** dictates the vertical exchange regime and therefore the frequency and intensity of nutrient replenishment events.
- **Sediment oxygen demand (SOD)** sets the redox boundary and drives hypolimnetic DO depletion.
- **Sediment phosphorus release (PO4R)** governs the magnitude of internal nutrient regeneration during stratified periods.
- **Extinction coefficients (EXA, EXM, EXOM, EXSS)** moderate the competition between light availability and thermal stability.

During calibration, parameters controlling **mixing and internal fluxes** should receive higher priority than those affecting external loads, as they explain most of the seasonal and inter-annual variability. These sensitivities also guide realistic constraint ranges for subsequent scenario analyses—e.g., climate-driven changes in mixing depth or sediment flux intensity.

4.4 Comparison to Regional Lake Models

To place the model's behavior within a regional limnological context, the sensitivity profile of Lake Osakis was compared to published CE-QUAL-W2 models for two other central Minnesota lakes: Madison Lake and Pearl Lake (Smith et al., 2014; Smith, 2019). The comparative sensitivity of key parameters across these three systems is detailed in Table 25.

Table 25. Sensitivity Comparison to two central Minnesota CE-QUAL-W2 Lake Models (Pearl and Madison Lakes).

Parameter Sensitivity	Madison Lake (Deep, Dimictic)	Pearl Lake (Shallow, Polymictic)	Lake Osakis (Deep, Dimictic)
Wind Exposure (WSC)	High Impact. A ±20% change in WSC leads to a 22.8% change in deep-water DO.	High Impact. Shows a -21.1% change in deep-water DO, indicating a strong link between wind, mixing, and oxygen.	High Impact. Drives a ~17% change in DO, confirming wind is a primary control on mixing and reaeration.
Sediment Oxygen Demand (SOD)	High Impact. Causes a ±10.8% change in deep-water DO.	Moderate Impact. Shows a ±7.4% change, indicating it is less dominant than in deeper lakes.	High Impact. Drives a -30% decline in DO, establishing the anoxic conditions for nutrient release.

Internal Phosphorus Loading (PO_4R)	High Impact. Drives a ±6.9% change in total phosphorus.	High Impact. Drives a ±11.3% change in total phosphorus.	High Impact. Directly alters phosphorus and algal concentrations, causing a +25% change in PO_4.
Light Limitation (EXH_2O, EXSS)	Moderate.	High.	Moderate.

4.4.1 Summary of Comparison

As shown in the comparative metrics in Table 25, the calibrated Lake Osakis model behaves consistently with other deep, dimictic lakes in the region that are subject to strong internal loading.

- Similarity to Madison Lake: Both Lake Osakis and Madison Lake are deep, stratifying systems where water quality is fundamentally driven by the interplay of wind mixing and sediment fluxes. Table 25 highlights this alignment, showing that both lakes exhibit high sensitivity to WSC, SOD, and PO_4R. An updated model for Madison Lake reinforces this, showing that internal loading accounted for 39% to 48% of the total phosphorus load (Smith, 2019)—a dynamic nearly identical to that observed in Lake Osakis.

- Contrast with Pearl Lake: As a shallower, polymictic (frequently mixed) lake, Pearl Lake is more sensitive to external factors and light limitation. This difference is quantified in Table 25, where Pearl Lake shows a "High" sensitivity to light limitation parameters, while Osakis and Madison are only "Moderate." Its dynamics are fundamentally different from the deep, stratified systems of Osakis and Madison.
- Conclusion for Lake Osakis: The relative rankings in Table 25 validate a key conclusion of this study: Lake Osakis behaves like Madison Lake, where internal processes are the dominant driver of summer water quality. This finding underscores that management strategies for Lake Osakis must address internal nutrient recycling to be effective, as watershed controls alone will be insufficient to overcome these powerful internal feedback loops.

5 Alternatives Analysis

The alternatives analysis was conducted using the calibrated and validated CE-QUAL-W2 model described in Sections 3 and 4. The model reproduces the dominant physical and biogeochemical processes governing Lake Osakis, including thermal stratification, internal nutrient cycling, suspended sediment transport, and phytoplankton dynamics. This provides a defensible framework for evaluating system response to watershed and in-lake management actions. Because the modeled alternatives influence both external loading pathways and internal feedback mechanisms, response was evaluated at multiple spatial and temporal scales rather than relying solely on whole-lake means.

The alternatives analysis was designed to address two related questions. The first was whether the modeled management actions improve whole-lake summer water quality relative to baseline conditions. The second was whether those improvements are driven primarily by reductions in watershed-derived loading, suppression of internal nutrient cycling, or both. To answer these questions, results were evaluated using paired-year comparisons, quantile-based metrics, annual variability summaries, zone-specific analyses, and distribution-based diagnostics. This combination of approaches allows direct interpretation of both average conditions and ecologically important upper- and lower-tail behavior.

5.1 Scenario Design

The evaluated alternatives represent a progression of management strategies targeting both external loading and internal nutrient cycling. The analyzed alternatives include the existing conditions (baseline alternative) and four proposed management actions that combine specific measures (Table 26).

Alternative 1 represents a scenario that includes an outlet modification plus a wetlands restoration measure. Alternative 2 builds off Alternative 1 by adding an agricultural management measure. Then separately, Alternatives 3 and 4 add in-lake treatments to Alternative 2, either an alum-type measure (Alternative 3) or a focused dredging measure (Alternative 4). The alternatives were constructed to reflect sensitivity analysis findings identifying sediment phosphorus release, light attenuation, and organic matter dynamics as primary controls on summer water quality. Each alternative was implemented in the CE-QUAL-W2 model by modifying the outlet configuration, and then the boundary conditions (HSPF loadings) and/or internal process coefficients consistent with the conceptual design of the measure. Each measure is fully described in the accompanying Lake Osakis Sediment Analysis and Comprehensive Plan (USACE, St. Paul District, 2026). All simulations used identical meteorological forcing, hydrology, and initial conditions to ensure that differences between scenarios reflect only the imposed management changes.

Table 26. Description of modeled alternatives and associated management actions

Measure	Alt 1	Alt 2	Alt 3	Alt 4	Baseline
Outlet Modification	Y	Y	Y	Y	N
Wetlands restoration	Y	Y	Y	Y	N
Focused dredging	N	N	N	Y	N
In-Lake Treatment (Alum)	N	N	Y	N	N
Ag Incentivization	N	Y	Y	Y	N

Performance was evaluated for the June–September stratified period, when hypolimnetic oxygen depletion, internal phosphorus release, and peak algal biomass are most pronounced. A paired-year comparison framework was used so that each alternative year was evaluated against the corresponding reference-condition year. This approach reduces the effect of interannual hydrologic and meteorological variability and provides a more defensible estimate of management effect than pooled comparisons alone.

The principal metrics used in the analysis were quantile-based and mean paired differences. These quantiles represent percentiles of occurrence: Q10 is the 10th percentile (representing low-end conditions), Q50 is the 50th percentile (representing median or typical conditions), and Q90 is the 90th percentile (representing high-end conditions). Dissolved oxygen was evaluated primarily using Q10 metrics to emphasize low-end, biologically stressful conditions. Secchi depth was evaluated using Q50 because median clarity is more representative of typical user experience than isolated extremes. Chlorophyll-a, phosphorus, turbidity, and suspended solids were evaluated primarily using Q90 and mean metrics to characterize both average seasonal response and upper-tail bloom or loading behavior. Bootstrap confidence intervals were used to evaluate the consistency of paired differences across years. Distribution-based statistics, including Kolmogorov–Smirnov and Wasserstein metrics, were used to determine whether scenario effects reflect only a modest shift in central tendency or a broader redistribution of water-quality behavior.

5.1.1 Watershed Scenario Implementation

The boundary conditions for the watershed management alternatives were developed by modifying the baseline HSPF model loads using the HSPF Scenario Application Management (HSPF-SAM) program. This tool allows for the simulation of various agricultural best management practices (BMPs) and land use changes to generate new inflow time-series for the CE-QUAL-W2 model.

- Alternative 1 (Wetlands Restoration): To simulate this scenario, 4,407.4 acres of cropland in the Judicial Ditch #2 (JD2) drainage area were treated with the wetland restoration BMP within HSPF-SAM. This acreage corresponds to the 21 specific sites identified for potential restoration. This action resulted in an average annual load reduction of 0.028 tons/ac/yr of sediment and 0.217 lbs/ac/yr of total phosphorus.
- Alternative 2 (Agricultural Incentivization): This scenario was simulated by applying a suite of agricultural BMPs to 1,600 acres of cropland within the lake's drainage area using HSPF-SAM. The specific practices modeled included Alternative Tile Inlets (700 acres), Controlled Tile Drainage (500 acres), Wetland Restoration (100 acres), and Tile Line Bioreactors (300 acres).

This detailed, model-based approach ensures that the boundary conditions used for each alternative are directly linked to the specific management actions being evaluated.

5.1.2 In-lake treatment

In-lake management actions for Alternatives 3 and 4 were simulated by adjusting the baseline sediment phosphorus release rate (PO4R) of 0.005 g/m2/day. These adjustments reflect the conceptual design, engineering analysis, and anticipated longevity of each measure:

- Alternative 3 (Alum Treatment): While alum provides a significant reduction in internal phosphorus loading, it is less permanent than physical sediment removal due to gradual aging and burial. To account for this over the 20-year simulation, the baseline PO4R in targeted segments was conservatively reduced to 0.0046 g/m2/day.

- Alternative 4 (Focused Dredging): Dredging physically removes sediment from high-priority areas identified by Houston Engineering, Inc. (HEI), which comprise approximately 14.02% of the lake area (Figure 66). To model this permanent reduction in internal loading, the baseline PO4R was reduced proportionally by 14.02%, resulting in a final rate of 0.0043 g/m2/day.

Figure 66. High-priority dredging areas identified for Alternative 4, comprising 14.02% of the total lake area

5.2 Whole-Lake Response

Whole-lake, baseline-referenced results indicate that all modeled alternatives improve summer water quality relative to existing conditions. The analysis demonstrates a consistent, logical progression of increasing water quality benefits as management strategies are layered during the critical June–September analysis period (1996–2015). These comprehensive whole-lake responses are detailed in Table 27.

Table 27. Simulated whole-lake summer response relative to baseline for Alternatives 1–4 during the June–September analysis period, 1996–2015.

Scenario	Dissolved Oxygen	Secchi Depth	Chlorophyll-a	Total Phosphorus	Phosphate	Total Suspended Solids	Turbidity
Alt 1	+0.264 mg/L	+0.153 m	-5.032 ug/L	-0.018 mg/L	-0.004 mg/L	-0.596 mg/L	-0.825 NTU
Alt 2	+0.300 mg/L	+0.172 m	-5.458 ug/L	-0.019 mg/L	-0.004 mg/L	-0.684 mg/L	-0.947 NTU
Alt 3	+0.315 mg/L	+0.181 m	-5.757 ug/L	-0.020 mg/L	-0.005 mg/L	-0.706 mg/L	-0.977 NTU
Alt 4	+0.329 mg/L	+0.189 m	-5.989 ug/L	-0.021 mg/L	-0.005 mg/L	-0.723 mg/L	-1.000 NTU

5.2.1 Whole-Lake Mitigation Dynamics

The modeling results presented in Table 27 reveal a clear distinction in how different management strategies affect the lake's water quality. The alternatives are structured sequentially, with in-lake treatments evaluated as distinct options applied on top of the optimal watershed framework:

- Watershed-Scale Controls (Alternatives 1 and 2): Alternative 1 (Wetlands Restoration) establishes a strong foundation by reducing external sediment and nutrient delivery, resulting in enhanced water clarity and improved dissolved oxygen regimes. Alternative 2 builds directly upon this foundation by incorporating agricultural best management practices (BMPs). This combined watershed approach provides further reductions in nutrient concentrations and algal biomass (chlorophyll-a) beyond what wetlands alone can achieve.

- In-Lake Treatments (Alternatives 3 and 4): To address internal nutrient loading, Alternatives 3 and 4 represent two distinct, mutually exclusive in-lake management options. Both scenarios assume the Alternative 2 watershed controls are already in place. Alternative 3 (Alt 2 + Alum Treatment) provides substantial reductions in internal phosphorus release, suppressing algal blooms compared to watershed controls alone. Alternative 4 (Alt 2 + Focused Dredging) physically removes targeted high-priority sediments, imposing a permanent cap on internal loading. This option outperforms the alum treatment, yielding the greatest overall benefit across all modeled parameters.

To visualize these relationships, a normalized response heatmap is presented in Figure 67. This comparative view underscores that while comprehensive watershed measures (Alternative 2) successfully address external loading, selecting an in-lake control—particularly dredging (Alternative 4)—is required to achieve the highest tier of water clarity and dissolved oxygen recovery.

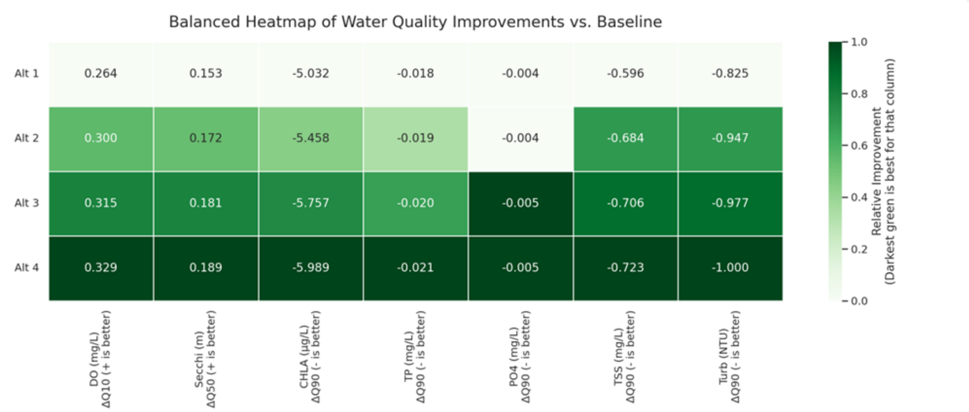

Figure 67. Whole-lake response heatmap showing baseline-referenced changes in key water-quality indicators for Alternatives 1–4. Note: Color gradients in this heatmap are scaled independently column-by-column to highlight relative performance changes within each specific metric, rather than being scaled globally across the entire chart.

5.3 Incremental Alternative Effects

The incremental comparison demonstrates that each successive management action contributes additional water-quality benefits. These incremental results, detailed in Tables 28 through 31, support the interpretation that watershed and in-lake measures are complementary rather than competing strategies.

Alternative 1 provides the initial watershed and outlet/wetland restoration benefit relative to baseline (Table 28. Incremental change in key water-quality parameters for Alternative 1 relative to baseline). This action establishes a strong foundation for whole-lake improvement across all evaluated metrics.

Table 28. Incremental change in key water-quality parameters for Alternative 1 relative to baseline

Constituent / Metric	Mean Change	95% CI	Years Improved
Dissolved Oxygen (Delta Q10)	+0.264 mg/L	+0.184 mg/L to +0.350 mg/L	17/20
Secchi Depth (Delta Q50)	+0.153 m	+0.142 m to +0.165 m	20/20
Chlorophyll-a (Delta Q90)	-5.032 ug/L	-5.759 ug/L to -4.316 ug/L	20/20
Total Phosphorus (Delta Q90)	-0.018 mg/L	-0.020 mg/L to -0.016 mg/L	20/20
Phosphate (Delta Q90)	-0.004 mg/L	-0.005 mg/L to -0.002 mg/L	19/20
Total Suspended Solids (Delta Q90)	-0.596 mg/L	-0.732 mg/L to -0.476 mg/L	20/20
Turbidity (Delta Q90)	-0.825 NTU	-1.029 NTU to -0.645 NTU	20/20

The transition from Alternative 1 to Alternative 2 results in modest but consistent reductions in nutrient concentrations, algal biomass, turbidity, and suspended solids, while improving water clarity and dissolved oxygen (Table 29). These results indicate that watershed nutrient and sediment reductions (Ag BMPs) remain beneficial even in a lake with substantial internal nutrient cycling.

Table 29. Incremental change in key water-quality parameters for Alternative 2 relative to Alternative 1

Constituent / Metric	Mean Change	95% CI	Years Improved
Dissolved Oxygen (Delta Q10)	+0.037 mg/L	+0.026 mg/L to +0.047 mg/L	17/20
Secchi Depth (Delta Q50)	+0.019 m	+0.018 m to +0.021 m	20/20
Chlorophyll-a (Delta Q90)	-0.425 ug/L	-0.507 ug/L to -0.347 ug/L	20/20
Total Phosphorus (Delta Q90)	-0.001 mg/L	-0.001 mg/L to -0.001 mg/L	20/20
Phosphate (Delta Q90)	-0.0004 mg/L	-0.001 mg/L to -0.0003 mg/L	19/20
Total Suspended Solids (Delta Q90)	-0.088 mg/L	-0.116 mg/L to -0.064 mg/L	20/20
Turbidity (Delta Q90)	-0.122 NTU	-0.164 NTU to -0.086 NTU	20/20

Alternatives 3 and 4 provide additional improvements beyond Alternative 2 by targeting internal nutrient processes. Alternative 3 reduces phosphorus availability through the alum treatment representation, resulting in further incremental benefits (Table 30).

Table 30. Incremental change in key water-quality parameters for Alternative 3 relative to Alternative 2.

Constituent / Metric	Mean Change	95% CI	Years Improved
Dissolved Oxygen (Delta Q10)	+0.014 mg/L	+0.010 mg/L to +0.019 mg/L	16/20
Secchi Depth (Delta Q50)	+0.009 m	+0.008 m to +0.011 m	20/20
Chlorophyll-a (Delta Q90)	-0.299 ug/L	-0.336 ug/L to -0.258 ug/L	20/20

Total Phosphorus (Delta Q90)	-0.001 mg/L	-0.001 mg/L to -0.001 mg/L	20/20
Phosphate (Delta Q90)	-0.001 mg/L	-0.001 mg/L to -0.001 mg/L	19/20
Total Suspended Solids (Delta Q90)	-0.022 mg/L	-0.025 mg/L to -0.019 mg/L	20/20
Turbidity (Delta Q90)	-0.030 NTU	-0.034 NTU to -0.025 NTU	20/20

Alternative 4 produces the largest simulated water-quality improvements, which reflects the physical differences between the two in-lake strategies. Because physical sediment removal (dredging) permanently extracts the organic, nutrient-rich muck from the lake, it provides a more complete and permanent reduction in internal loading over the 20-year model run. This physical mechanism was represented in the model by applying a lower sediment phosphorus release coefficient (PO4R of 0.0043 g/m2/day) to the dredged areas, compared to the chemical inactivation represented in Alternative 3 (PO4R of 0.0046 g/m2/day). These physical differences translate directly into superior water-quality metrics, with the specific incremental benefits of Alternative 4 (relative to Alternative 2) detailed in Table 31.

Table 31. Incremental change in key water-quality parameters for Alternative 4 relative to Alternative 2

Constituent / Metric	**Mean Change**	**95% CI**	**Years Improved**
Dissolved Oxygen (Delta Q10)	+0.028 mg/L	+0.020 mg/L to +0.037 mg/L	17/20
Secchi Depth (Delta Q50)	+0.017 m	+0.015 m to +0.019 m	20/20
Chlorophyll-a (Delta Q90)	-0.532 ug/L	-0.598 ug/L to -0.458 ug/L	20/20
Total Phosphorus (Delta Q90)	-0.002 mg/L	-0.002 mg/L to -0.002 mg/L	20/20
Phosphate (Delta Q90)	-0.001 mg/L	-0.002 mg/L to -0.001 mg/L	20/20
Total Suspended Solids (Delta Q90)	-0.039 mg/L	-0.045 mg/L to -0.033 mg/L	20/20
Turbidity (Delta Q90)	-0.052 NTU	-0.061 NTU to -0.044 NTU	20/20

5.4 Distributional Shift Analysis

While paired differences highlight changes in average and extreme conditions, Kolmogorov-Smirnov (KS) and Wasserstein metrics were calculated to verify if the management scenarios fundamentally altered the lake's overall water quality distribution.

For clarity, Table 32 summarizes these metrics for the recommended action (Alternative 4) across the primary constituents of concern. The KS test yielded statistically significant p-values ($p < 0.001$) across all major constituents, proving that the physical removal of sediment didn't just shift isolated daily averages, but successfully altered the entire ecological regime of the lake. The Wasserstein distances further quantify the magnitude of this shift.

Table 32. Distributional Statistics Summary: Recommended Alternative 4 (Dredging) vs. Baseline (Whole Lake)

Constituent	KS Statistic	KS p-value	Wasserstein Distance
Dissolved Oxygen	0.022	< 0.001	0.154
Secchi Depth	0.160	< 0.001	0.183
Chlorophyll-a	0.148	< 0.001	3.547
Total Phosphorus	0.403	< 0.001	0.020
Total Suspended Solids	0.151	< 0.001	0.530

5.5 Zone-Specific Response

While the whole-lake summaries provide a synoptic view of system improvement, evaluating water quality exclusively at the whole-lake scale can obscure the localized benefits of targeted management actions. Because Lake Osakis exhibits distinct spatial dynamics—such as localized tributary loading in the bays and intense internal nutrient recycling in the deep basins—it is critical to evaluate how specific alternatives perform in the zones they were designed to treat.

Table 33 distills the comprehensive spatial model output down to the primary performance indicators for two critical management zones: Branch 2 (Miller Bay), which receives substantial external loading from Judicial Ditch #2, and the Dynamic Hypolimnion, where internal sediment phosphorus release is most concentrated.

Table 33. Summary of primary zone-specific responses for key management alternatives relative to baseline conditions.

Lake Zone	Primary Performance Metric	Alt 1 (Wetlands)	Alt 2 (Ag BMPs)	Alt 3 (Alum)	Alt 4 (Dredging)
Branch 2	Turbidity (Delta Q90)	-1.583 NTU	-1.570 NTU	n/a*	-1.570 NTU
Branch 2	Total Suspended Solids (Delta Q90)	-1.096 mg/L	-1.087 mg/L	n/a*	-1.087 mg/L
Dynamic Hypolimnion	Phosphate (Delta Q90)	n/a*	n/a*	-0.004 mg/L	-0.006 mg/L
Dynamic Hypolimnion	Dissolved Oxygen (Delta Q10)	n/a*	n/a*	0.000 mg/L	0.000 mg/L

**n/a indicates that the modeled scenario does not contain a primary management mechanism designed to act on this specific zone/metric interaction.*

Branch 2 functions as the primary receiving water for external sediment and nutrient loads delivered by the watershed. As shown in Table 33, the watershed-focused frameworks (Alternatives 1 and 2) produce substantial, localized improvements in Branch 2 turbidity and suspended solids. The in-lake treatments (Alum/Dredging) are marked "n/a" for this zone because they are applied to the main lake body and do not possess a physical mechanism to intercept incoming watershed sediment. This confirms that robust watershed management is the necessary and most effective strategy for mitigating localized impairments in the tributary bays.

Conversely, the dynamic hypolimnion represents the deep, seasonally anoxic bottom waters where internal phosphorus loading is most severe. Alternatives 1 and 2 (watershed controls) are marked "n/a" for this zone because they do not directly alter the sediment chemistry. In contrast, both in-lake treatments (Alternatives 3 and 4) successfully suppress the release of phosphate from the sediments, with dredging (Alt 4) proving to be the most effective strategy. Notably, the model indicates that the hypolimnion will still experience severe anoxia (0.000 mg/L Dissolved Oxygen) under all scenarios. This confirms that physical or chemical intervention in the sediments is an absolute requirement for controlling internal phosphorus loading, as the redox conditions that drive that release will persist even with maximum watershed improvements.

5.6 Annual Variability and Robustness

The 1996–2015 baseline period was utilized because it captures a highly representative range of historical hydrological conditions, successfully encompassing both extreme wet (flood) and dry (drought) years. This ensures that the model's alternatives have been rigorously stress-tested against long-term climate and flow variability.

Annual paired comparisons (Table 34) indicate that the alternatives generally improve conditions across most years rather than being driven by a small number of hydrologic events. This is important because Lake Osakis has a long hydraulic residence time and strong internal nutrient feedbacks. Consistent annual improvement provides stronger support for management effectiveness than a single pooled seasonal mean alone, as illustrated by the robust, year-over-year improvement trends for key metrics shown in Figure 68.

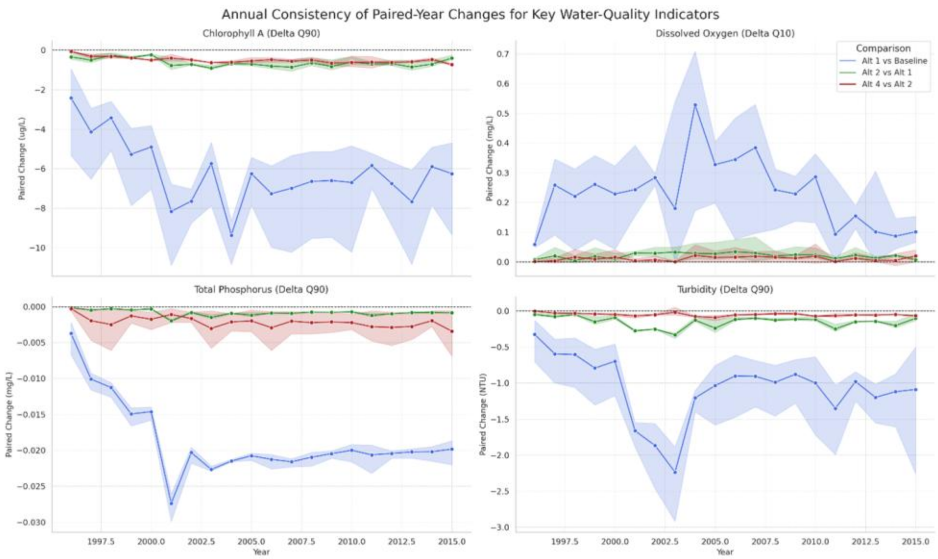

Figure 68. Annual consistency of paired-year changes for key water-quality indicators.

Table 34. Annual variability summary for selected paired-year metrics across the 1996-2015 analysis period.

Comparison	Metric	Mean change	Years improved	Years adverse
Alt 1 vs Baseline	Chlorophyll-a Delta Q90	-5.032 ug/L	20/20	0/20
Alt 1 vs Baseline	Dissolved Oxygen Delta Q10	+0.264 mg/L	17/20	0/20
Alt 1 vs Baseline	Total Phosphorus Delta Q90	-0.018 mg/L	20/20	0/20
Alt 2 vs Baseline	Chlorophyll-a Delta Q90	-5.458 ug/L	20/20	0/20
Alt 2 vs Baseline	Dissolved Oxygen Delta Q10	+0.300 mg/L	17/20	0/20
Alt 2 vs Baseline	Total Phosphorus Delta Q90	-0.019 mg/L	20/20	0/20

Alt 3 vs Baseline	Chlorophyll-a Delta Q90	-5.757 ug/L	20/20	0/20
Alt 3 vs Baseline	Dissolved Oxygen Delta Q10	+0.315 mg/L	17/20	0/20
Alt 3 vs Baseline	Total Phosphorus Delta Q90	-0.020 mg/L	20/20	0/20
Alt 4 vs Baseline	Chlorophyll-a Delta Q90	-5.989 ug/L	20/20	0/20
Alt 4 vs Baseline	Dissolved Oxygen Delta Q10	+0.329 mg/L	17/20	0/20
Alt 4 vs Baseline	Total Phosphorus Delta Q90	-0.021 mg/L	20/20	0/20
Alt 2 vs Alt 1	Chlorophyll-a Delta Q90	-0.425 ug/L	20/20	0/20
Alt 2 vs Alt 1	Dissolved Oxygen Delta Q10	+0.037 mg/L	17/20	0/20
Alt 2 vs Alt 1	Total Phosphorus Delta Q90	-0.001 mg/L	20/20	0/20
Alt 3 vs Alt 2	Chlorophyll-a Delta Q90	-0.299 ug/L	20/20	0/20
Alt 3 vs Alt 2	Dissolved Oxygen Delta Q10	+0.014 mg/L	16/20	1/20
Alt 3 vs Alt 2	Total Phosphorus Delta Q90	-0.001 mg/L	20/20	0/20
Alt 4 vs Alt 2	Chlorophyll-a Delta Q90	-0.532 ug/L	20/20	0/20
Alt 4 vs Alt 2	Dissolved Oxygen Delta Q10	+0.028 mg/L	17/20	0/20
Alt 4 vs Alt 2	Total Phosphorus Delta Q90	-0.002 mg/L	20/20	0/20

5.7 Integrated Interpretation

The alternatives analysis indicates that watershed and in-lake management actions are complementary. Alternative 1 improves conditions relative to baseline by reducing external loading and modifying the hydrologic/wetland framework. Alternative 2 adds agricultural load reductions and produces further improvement. Alternatives 3 and 4 then address internal nutrient cycling more directly, producing additional water-quality benefits on top of the Alternative 2 framework.

The supporting nutrient table (Table 35) broadens this interpretation beyond phosphorus alone. Although phosphorus and chlorophyll-a remain the principal eutrophication indicators, the consistent nitrogen reduction helps confirm that the alternatives are altering the overall nutrient pool behavior.

Table 35. Supporting nutrient-response summary for total nitrogen, ammonium, and nitrate-nitrite.

Scenario	Total Nitrogen	Ammonium	Nitrate-Nitrite
Alt 1	-0.277 mg/L	-0.025 mg/L	-0.007 mg/L
Alt 2	-0.287 mg/L	-0.028 mg/L	-0.008 mg/L
Alt 3	-0.293 mg/L	-0.028 mg/L	-0.008 mg/L
Alt 4	-0.298 mg/L	-0.028 mg/L	-0.008 mg/L

The strongest modeled response was produced by Alternative 4. This result is consistent across the whole-lake summary, the incremental comparisons, the zone-specific data, and the distribution-based diagnostics. Alternative 4 combines watershed measures, agricultural load reductions, and focused dredging, thereby comprehensively addressing both external loading and internal phosphorus feedbacks. This combined mechanism is the most effective approach for improving the complex, multi-scale water quality dynamics of Lake Osakis.

Ultimately, while Alternative 4 clearly demonstrates the highest ecological benefit and greatest overall improvement to lake water quality, the final selection of a management alternative will require pairing these modeled environmental improvements with a comprehensive economic cost-benefit analysis.

6 Alternatives Discussion

The alternatives analysis demonstrates that water quality response in Lake Osakis is governed by the coupled interaction among external loading, internal nutrient cycling, thermal stratification, and light availability. No single metric or lake zone is sufficient to characterize management effectiveness. Instead, the alternatives should be judged by their combined influence on whole-lake conditions, upper-water-column clarity and algal response, bottom-water nutrient regeneration, and consistency across years.

The model results support a management approach that combines external load reduction with targeted in-lake treatment. Watershed measures alone provide measurable improvements, and agricultural load reductions further improve on the outlet/wetland framework. However, the largest overall modeled response occurs when in-lake treatment is added to the watershed framework. This reflects the importance of internal nutrient cycling in Lake Osakis during the summer stratified period.

Ultimately, the results demonstrate a sequential accumulation of benefits: Alternative 2 improves upon the foundation of Alternative 1, while Alternatives 3 and 4 provide the highest level of water quality enhancement by addressing internal loading on top of the Alternative 2 watershed framework.

Among the modeled alternatives, Alternative 4 produced the strongest overall response across the majority of evaluated metrics. It reduced chlorophyll-a, phosphorus, suspended solids, and turbidity more than the other alternatives while also improving Secchi depth and dissolved oxygen relative to baseline. Therefore, Alternative 4 is identified as the recommended modeled alternative to align with the overarching management goals.

7 Conclusions

7.1 Model Summary and Fitness for Purpose

The successful development, calibration, and validation of the Lake Osakis CE-QUAL-W2 model provides the U.S. Army Corps of Engineers and the Sauk River Watershed District with a powerful and scientifically defensible tool for water quality management. Validated over a 20-year period (1996-2015), the model effectively represents the key physical and biogeochemical processes that define the lake's ecosystem.

While the model has known limitations in predicting the absolute peak of algal blooms, its performance in simulating physical parameters (temperature, stratification), foundational nutrients (orthophosphate, nitrate), and the relative response of the algal community is strong. The model is therefore a sound and appropriate tool for its intended purpose: evaluating the comparative effectiveness of different management scenarios to improve water quality in Lake Osakis.

7.2 Key Findings

The primary findings of this comprehensive modeling effort are conclusive:

1. Internal Processes Dominate Water Quality: The lake's water quality is predominantly driven by internal nutrient cycling, not short-term external loads. The lake's long hydraulic residence time (~5 years) buffers the immediate impact of watershed inputs, making internal feedback loops the primary control on summer water quality.
2. Anoxia is the Critical Driver: The model confirms that summer thermal stratification leads to hypolimnetic anoxia. This oxygen depletion is the critical trigger for the release of sediment-bound phosphorus, which provides the fuel for late-summer algal blooms.
3. A Combined Management Approach is Required: The analysis demonstrates that while watershed controls are essential for long-term lake health and clarity, they alone are not sufficient to overcome the powerful influence of internal loading.

7.3 Recommended Management Strategy

Based on the integrated interpretation of the alternatives analysis, the most effective restoration strategy for Lake Osakis is a combined approach that leverages the strengths of both watershed and in-lake treatments.

It is recommended that stakeholders prioritize Alternative 4, which comprehensively pairs foundational watershed improvements and agricultural load reductions with the targeted internal load reduction of focused dredging. This optimized approach is projected to yield the greatest overall benefit, preserving the clarity and habitat improvements from watershed controls while simultaneously achieving the strongest possible reduction in internal phosphorus recycling and the resulting nuisance algal blooms.

8 References

Chapra, S. C. 1997. *Surface Water-Quality Modeling.* McGraw-Hill.

Duan, Q., Sorooshian, S., & Gupta, V. 1992. "Effective and efficient global optimization for conceptual rainfall-runoff models." *Water Resources Research* 28 (4): 1015-1031.

Matsumoto. 2021. "MESMO 3: Flexible phytoplankton stoichiometry and refractory dissolved organic matte." *Geoscientific Model Development.*

Nürnberg, G. K. 1984. "The prediction of internal phosphorus loading in lakes with anoxic hypolimnia." *Limnology and Oceanography* 29 (1): 111-124.

Redfield, A. C. 1958. "The biological control of chemical factors in the environment." *American Scientist* 46 (3): 205-221.

Smith, E.A., and Kiesling, R.L. 2019. *Updates to the Madison Lake (Minnesota) CE–QUAL–W2 water-quality model for assessing algal community dynamics: U.S. Geological Survey Scientific Investigations Report 2019–5124.* Scientific Investigations Report, U.S. Geological Survey, 35 p. https://doi.org/10.3133/sir20195124.

Smith, E.A., Kiesling, R.L., and Ziegeweid. 2014. *Water-quality models to assess algal community dynamics, water quality, and fish habitat suitability for two agricultural land-use dominated lakes in Minnesota.* Scientific Investigations Report 2017–505, U.S. Geological Survey, U.S. Geological Survey, 65 p. https://doi.org/10.3133/sir20175056.

SRWD. 2023. *Osakis Lake Area Excess Nutrients Total Maximum Daily Load Report.* TMDL Report, Minnesota Pollution Control Agency.

Wells, S. A. 2017. *CE-QUAL-W2: A Two-Dimensional, Laterally Averaged, Hydrodynamic and Water Quality Model, Version 4.1 User Manual.* Department of Civil and Environmental Engineering, Portland State University.

Wells, Scott A. and Cole, T. ed. by S. Wells. 2025. *A Two-Dimensional, Laterally Averaged, Hydrodynamic and Water Quality Model, Version 4.5.* Department of Civil and Environmental Engineering, Portland State University, Portland, OR.

9 Appendices

9.1 Model Stability and Mass Balance Error

At the completion of the 20-year (1996-2015) simulation, the model's internal mass, water, and energy balance calculations were reviewed to ensure numerical stability. The CE-QUAL-W2 model performs this check by comparing the final amount of a substance in the model (spatial change) to the total amount that entered, left, and was produced or consumed over time (temporal change).

Summary of Model Error:

The results confirm that the model maintained an excellent mass balance for water, energy, and all simulated water quality constituents over the entire 20-year period.

Water Balance Error: The overall water balance error for the entire lake system was -0.000000035%.

Energy Balance Error: The overall energy (heat) balance error was 0.00000011%.

Mass Balance Error: For all individual water quality constituents (such as TDS, Phosphate, and Algae), the mass balance percent error was consistently on the order of 10^{-6} % to 10^{-7} %.

Interpretation:

These extremely low error values indicate that the model's numerical solver was stable and that there were no significant artificial gains or losses of mass or energy over the two-decade simulation. For example, an error of 10^{-6} % is equivalent to one part in one hundred million.

This confirms that the model's hydrodynamic and water quality calculations are numerically sound, providing high confidence that the simulation results are a valid representation of the system's biogeochemical processes, free from significant numerical artifacts.

Evaporation Summary

Branch	Mean Evaporation Rate (m^3/s)	Cumulative Evaporation (m^3)
Branch 1	0.585	416,412,143
Branch 2	0.020	14,237,585

Water and Energy Balance Error

Balance Type	Component	Percent Error (%)
Water	Waterbody 1 (Total)	-3.50×10^{-8}
	Branch 1	-3.44×10^{-8}
	Branch 2	-5.39×10^{-8}

Energy	Waterbody 1 (Total)	1.08×10^{-7}
	Branch 1	1.04×10^{-7}
	Branch 2	3.62×10^{-7}

Constituent Mass Balance Error (%)

Constituent	Branch 1 Error (%)	Branch 2 Error (%)
TDS	-1.83×10^{-7}	-5.44×10^{-7}
ISS	4.55×10^{-8}	1.22×10^{-6}
Phosphate	-2.54×10^{-7}	-6.88×10^{-7}
Ammonium	-5.01×10^{-7}	-3.38×10^{-6}
Nitrate-Nitrite	-1.75×10^{-7}	-3.54×10^{-7}
Labile DOM	-1.27×10^{-7}	-6.27×10^{-7}
Refractory DOM	-1.79×10^{-7}	-5.51×10^{-7}
Labile POM	4.27×10^{-7}	2.29×10^{-6}
Refractory POM	-1.43×10^{-8}	5.96×10^{-6}
Algae	9.32×10^{-8}	-1.65×10^{-7}
Dissolved Oxygen	-1.90×10^{-7}	-5.88×10^{-7}

9.2 PO4 FLUX Study- HEI, 2024

Methodology of Comparison

1. Observed Data: The HEI study provided several field measurements of PO4 flux from lake sediments. The report uses a representative value from these observations, specifically 4.73 mg/m²/day (or 0.00473 g/m²/day) for comparison.
2. Calculated Flux: This observed rate was multiplied by the bottom area of specific model segments to calculate an expected total daily PO4 flux in kilograms per day (kg/d).
3. Simulated Flux: This calculated value was then compared to the model's own simulated output for total PO4 flux from sediment (Simulated PO4SOD) for the same segments.

Comparison Results

Here is the breakdown of the comparison for the sites you mentioned:

- Lindberg (Segment 6):
    - Calculated Flux (using the observed rate): 0.104 kg/d
    - Simulated Peak Flux (from model output charts): Approximately 0.11 kg/d
    - *Analysis:* The simulated and calculated values are in very close agreement, suggesting the model is replicating the sediment phosphorus release well in this area.
- Four Mile Hole 209 (Segment 16):
    - Calculated Flux (using the observed rate): 0.048 kg/d
    - Simulated Peak Flux (from model output charts): Approximately 0.033 kg/d
    - *Analysis:* While not as closely matched as the Lindberg site, these values are reasonably similar and in the same order of magnitude. This provides confidence that the model's simulation is within a realistic range.
- Four Mile Hole 102 (Segment 14):
    - Calculated Flux (using the observed rate): 0.027 kg/d
    - Simulated Peak Flux: (from model output charts): Approximately 0.030 kg/d
    - *Analysis:* The simulated and calculated values are in very close agreement, suggesting the model is replicating the sediment phosphorus release well in this area.

In summary, despite the spatial differences between field measurements and model geometry, the comparison indicates that the model's calibrated sediment phosphorus release rate produces results that align well with expectations derived from observed data. The close match at the Lindberg site and Four Mile Hole 102 site and the reasonable agreement at the Four Mile Hole 209 site validate the model's simulation of this critical internal loading process.

Orange = Summer Sampling points
Blue = Winter Sampling points

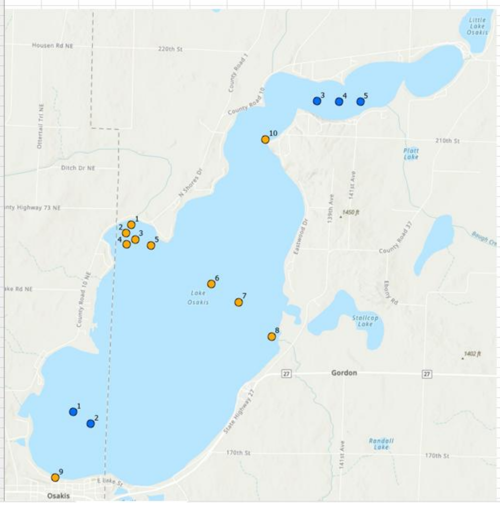

	1	2	3	4	5	6	8	9	10
Incubation period, d	0-8	2-8	0-8	0-8	0-8	2-8	2-8	3-8	2-8
Flux, mg/m2 d	9.68	5.31	7.95	4.73	5.20	0.95	0.09	1.79	2.91
Flux, g/m2 d	0.0097	0.0053	0.0080	0.0047	0.0052	0.0010	0.0001	0.0018	0.0029

Winter Sampling	Station				
	1	2	3	4	5
Incubation period, d	0-10	2-10	2-10	5-10	0-10
Flux, mg/m2 d	**5.34**	**2.96**	**2.44**	**4.30**	**2.27**

	Assuming Flux of 4.73 mg/m2 d					
Segment	Width M	length m	m2	Segment	kg/m2 d	kg/d
Lindberg	31	707	21917	6	4.73E-06	**0.104**
4mile 102	14	403	5642	15	4.73E-06	**0.027**
4mile 209	25	403	10075	16	4.73E-06	**0.048**

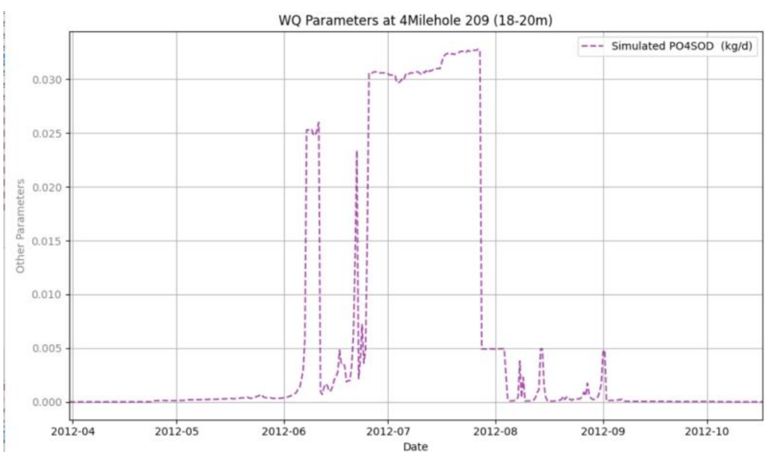

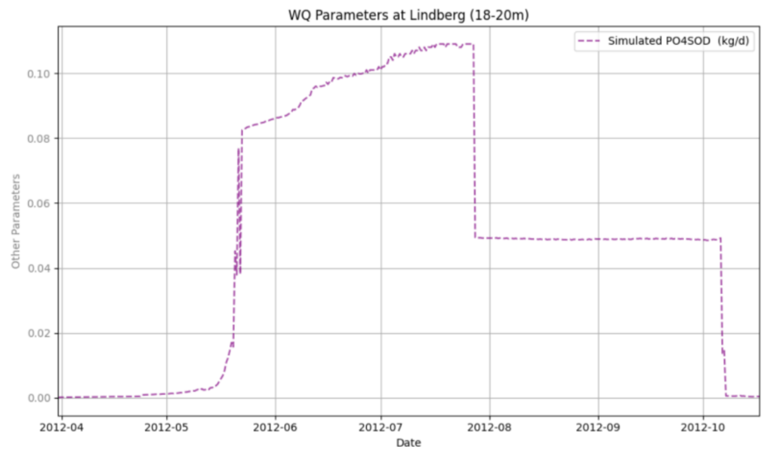
WQ Parameters at Lindberg (18-20m)
Simulated PO4SOD (kg/d)
Other Parameters
0.00
0.02
0.04
0.06
0.08
0.10
2012-04
2012-05
2012-06
2012-07
2012-08
2012-09
2012-10
Date

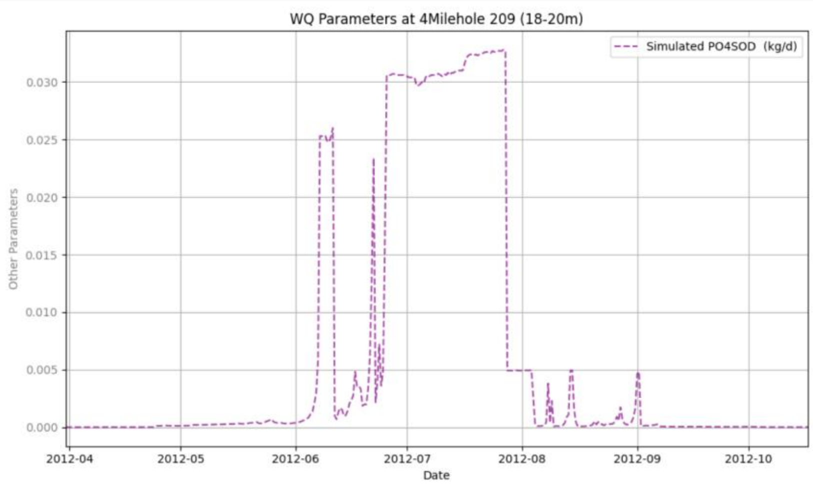
WQ Parameters at 4Milehole 209 (18-20m)
Simulated PO4SOD (kg/d)
Other Parameters
0.000
0.005
0.010
0.015
0.020
0.025
0.030
2012-04
2012-05
2012-06
2012-07
2012-08
2012-09
2012-10
Date